

ENGR7019 Engineering Dissertation Project Final Report



Artificially Informed Data Driven Physics Based Battery Model Parameterisation with Particle Swarm Optimisation (PSO) method for the LG M50 dataset

Nick Muir 17053998

Programme: MSc Automotive Engineering with Electric Vehicles

Module: ENGR7019

Academic year: 2021/2022

Word count	Main part	Appendix
	6232	5585
Number of illustrations	Main part	Appendix
	21	14

School of Engineering, Computing and Mathematics

Statement of originality

Except for those parts in which it is explicitly stated to the contrary, this project is my own work. It has not been submitted for any degree at this or any other academic or professional institution.

Nick Muir

03/08/2022

Signature of Author

Date

Regulations Governing the Deposit and Use of Master of Science Dissertations in the School of Engineering, computing and Mathematics, Oxford Brookes University.

1. The 'top' copies of projects submitted in fulfilment of Master of Science course requirements shall normally be kept by the Department.
2. The author shall sign a declaration agreeing that, at the supervisor's discretion, the dissertation may be submitted in electronic form to any plagiarism checking service or tool.
3. The author shall sign a declaration agreeing that the dissertation be available for reading and copying in any form at the discretion of either the project supervisor or in their absence the Head of Postgraduate Programmes, in accordance with 5 below.
4. The project supervisor shall safeguard the interests of the author by requiring persons who consult the dissertation to sign a declaration acknowledging the author's copyright.
5. Permission for anyone other than the author to reproduce in any form or photocopy any part of the dissertation must be obtained from the project supervisor, or in their absence the Head of Postgraduate Programmes, who will give his/her permission for such reproduction only to the extent which he/she considers to be fair and reasonable.

I agree that this dissertation may be submitted in electronic form to any plagiarism checking service or tool at the discretion of my project supervisor in accordance with regulation 2 above.

I agree that this dissertation may be available for reading and photocopying at the discretion of my project supervisor or the Head of Postgraduate Programmes in accordance with regulation 5 above.

Nick Muir

22/09/2022

Signature of Author

Date

Abstract

This thesis looks to provide the first ever Julia coded PBM optimisation toolbox utilising a PSO method and DFN model, this is a revolutionary piece of open-source software which enables a user to input measured cell data for an LGM50 and determine the physical and chemical parameters of a DFN model. At a larger scale this program could look to inform SOC and SOH prediction for the LGM50 by potentially using emulated higher fidelity terminal voltage responses and provide a better approximation of the physical and chemical parameters of a battery model than expensive experimental techniques.

The thesis firstly outlines a 6-stage methodology including literature reviews and software exploration. Then targets the 6 most sensitive parameters and confirms by performing an OAT analysis that the thickness of the cathode is the most sensitive parameter for terminal voltage behaviour for a HPPC and GITT test cycle within the virtual PBM environment of an LGM50 cell.

The thesis secondly builds and deploys an artificially informed optimisation to this virtual PBM environment and can improve the fitment of terminal voltage for a WLTP by 38% from an experimentally populated dataset for the LGM50. Which achieves a minimised voltage RMSE of 9.7mV with complete simulation time of ~1.5 hours averaging 8 seconds per WLTP drive cycle.

In conclusion, the thesis provides an open-source toolbox which is unique and powerful at fitting terminal voltage response for an LGM50.

Key words: LGM50, PSO, DFN, Julia, HPPC, GITT, WLTP, OAT, RMSE and PBM

Highlights

- The first ever Julia coded PBM parameter AI Optimisation tool using PETLION.jl and Metaheuristic.jl which are completely open-source packages to ensure wide utilisation.
- Built a working PSO method applied to a PBM optimisation for a DFN.
- User defined electrochemical dataset and custom functions for the Chen2020 LGM50 dataset within the domain of PETLION.
- Used experimental, simulated and measured data for the LGM50 to determine the validity of the developed model.

Acknowledgments

Throughout the writing of this thesis, I have received plenty of continued support and assistance. I would first like to thank my supervisors, Brady Planden and Katie Lukow, whose expertise and mentorship was invaluable in formulating the research topic and provided excellent modelling assistance.

Secondly, I want to thank HVES, who is the research group who will look to inherit my work. HVES kindly supplied the data for the LGM50 and again supported me through the challenging modelling aspects of the thesis.

Thirdly, I want to thank the Oxford Brookes Racing team. The team supported me to succeed with my thesis and allowed me to cultivate skills in EV technology. In which I could first hand see the long-term benefit of the work of my thesis and formulate the background to the opportunity.

Finally, I wish to thank my close family, in which they showed their unwavering support in the challenging moments of this thesis.

Table of Contents

Abstract	3
Highlights	4
Acknowledgments	4
List of Figures	7
List of Tables	8
List of Symbols and Abbreviations	9
1 Introduction and Background	10
1.1 Projects aim and objectives	11
1.2 Originality and Contributions	11
2 Literature review	12
2.1 ECM compared to P2D	12
2.2 Sensitivity Analysis	13
2.3 Data-driven Optimisation	14
2.4 PSO Optimisation	16
3 Methodology	17
3.1 Objective 1	18
3.2 Objective 2	18
3.3 Objective 3	19
3.3.1 PyBaMM	20
3.3.2 PETLION	20
3.4 Objective 4	21
3.4.1 Pyswarm	21
3.4.2 Optim.jl	21
3.4.3 Metaheuristics.jl	21
3.5 Objective 5	22
3.6 Objective 6	22

4	Results and Discussion	23
4.1	Temperature sensitivity to Terminal Voltage	23
4.2	Further sensitivity analysis	25
4.3	AI Optimisation	29
5	Conclusions	33
6	References	35
A.1	Detailed background	38
A.2	Detailed literature review	39
A.3	Methodology	46
A.4	Alternative approaches	53
A.5	Project limitations	54
A.6	Results and discussion	55
A.7	References	61
A.8	Bibliography	63

List of Figures

Figure 1: Commonly used battery electrical equivalent circuit models (Zhang, Xia, Li, Cao, et al., 2018)	12
Figure 2: P2D Porous-Electrode model (Plett, 2015)	12
Figure 3: Schematic of experiment-based parameter identification (Li et al., 2022)	14
Figure 4: Schematic of the multi-objective multi-step data-driven identification process (Li et al., 2022)	14
Figure 5: Error distributions of the invasive experimental and data-driven parameter	15
Figure 6: PSO against CSA for simulation iterations and RMSE voltage error (Li et al., 2022)	16
Figure 7: Overall Project Methodology	17
Figure 8: Chen2020 dataset simulating a 2C discharge comparing SPM, SPM _e and DFN (Planella et al., 2022)	20
Figure 9: Benchmarking of PETLION, LIONSIMBA and PyBaMM (Berliner et al., 2021)	20
Figure 10: Overriding methodology for entire model	22
Figure 11: Average Sensitivity in Temperature for GITT (a) and HPPC (b) for LCO dataset	23
Figure 12: GITT (blue) and HPPC (green) RMSE voltage for temperature OAT with the orange line denoting benchmark temperature of 25°C for LCO	24
Figure 13: GITT comparison of real-world LGM50 data against PETLION simulated voltage and C-rate	25
Figure 14: RMSE in Terminal voltage for I_p (a), ϵ_p (b), I_n (c), k_n (d), $C_{max,p}$ (e) and ϵ_n (f) for GITT, where the Orange line denotes the original point of the LGM50 dataset	26
Figure 15: Ranking of Parameter Sensitivity for the LGM50 dataset within PETLION	28
Figure 16: Global particles swarm with the fitness of the RMSE voltage at initialisation (a) and at 10th generation (b)	29
Figure 17: WLTP response driven by PSO optimization	32

Appendix List of Figures

Figure 18: ECM against a PBM from MPC analysis (G. Florentino and M. S Trimoli, 2018)	39
Figure 19: Visual Comparison of different sensitivity analysis weighting magnitude of sensitivity (Andersson et al., 2022)	43
Figure 20: Classification of a subset of optimization methods that has been used for PBM (Andersson et al., 2022)	44
Figure 21: Process for OAT sensitivity analysis	46
Figure 22: HPPC comparison of real-world LGM50 data against PETLION simulated voltage and C-rate	55
Figure 23: WLTP comparison of real-world LGM50 data against PETLION simulated voltage and C-rate	55
Figure 24: Time series sampled comparison for GITT, PETLION is original and Measured data is down sampled	57
Figure 25: Example of Terminal Voltage changing with OAT L_n	59

List of Tables

Table 1: Correlation and RMSE of Drive cycles from PETLION to Measured Data for LGM50	25
Table 2: PSO results for PETLION Virtual Validation for GITT.....	30
Table 3: PETLION PSO results for measure data WLTP	31

Appendix List of Tables

Table 4: Comparison of 2D PBM methods	41
Table 5: Accessed Software tools summary.....	47
Table 6: Proposed boundary conditions for PETLION OAT for 6 strongest parameters.....	49
Table 7: Chen2020 parameters required for PETLION DFN.....	51
Table 8: Alternatives approaches for project objectives	53
Table 9: Overall Project Limitations	54
Table 10: PETLION PSO results for measure data 'GITT' and WLTP	60

List of Symbols and Abbreviations

BJDST	Beijing Dynamic Stress Test
BMS	Battery Management Systems
CC-CV	Constant Current – Constant Voltage
C-rate	Ratio of Current related to Cell Capacity
DAE's	Differential-Algebraic System of Equations
DFN	Doyle Fuller Newman
DOD	Depth Of Discharge
DST	Dynamic Stress Test
ECM	Equivalent Circuit Model
GITT	Galvanostatic Intermittent Titration Technique
HPPC	Hybrid Pulse Power Characterization
LCO	Lithium Cobalt Oxide
MIL	Model In Loop
OCP	Open Circuit Potential
OCV	Open Circuit Voltage
P2D	Pseudo-two-dimensional
PBM	Physical Based Battery Model
PDE	Partial Differential Equations
PSO	Particle Swarm Optimisation
SEI	Solid Electrolyte Interphase
SOC	State Of Charge
SOH	State Of Health
WLTP	Worldwide Harmonised Light Vehicle Test Procedure

1 Introduction and Background

Rechargeable batteries are everywhere and can be scaled in different sizes for different applications, in instance at the Wh level they are used in mobile phones, kWh level they are in Electric Vehicles and MWh level they are used for off grid energy storage. Currently, Lithium-ion batteries are the dominant chemistry available on the market due to their high power and energy densities, but there is ongoing research to find more cost effective solutions to be more consumer focused and ensure better affordability for battery powered items (Mehta, 2022).

In order to improve this the modelling of batteries is critical, as this enables a system to be better understood and optimised without the dependency of constant experiments, so multiple hypotheses can be tested and validated faster and with less capital expenditure. These modelling approaches can be applied in varying levels from just at the individual cell to discover new chemistries or to improve functional safety of a BMS by understanding the true SOC and SOH limits of large battery packs (Synopsys, 2022).

Primarily, this thesis will investigate the modelling methods at the individual cell level in the physical and chemical domain and look to build a system which can optimise and find these parameters from a well understood academic dataset called Chen2020 which is from the LG M50 (Chen *et al.*, 2020). PBM's are vastly complex and require high computational effort to determine the complex chemical interactions, so the dependency on data-driven Artificial Intelligence (AI) is critical to correlate fitment of new result against a known baseline quickly and efficiently.

This form of research is completely new field, so any step which requires less computational effort or time to get high fitting results is highly advantageous to the industry.

1.1 Projects aim and objectives

The main aim of the project is to develop an AI model that will optimise the 6 highest sensitivity physical based parameters for battery cells with a PSO method, this is achieved by focusing on what constitutes these 6 of the 26 parameters that drive cell characteristics for a PBM. This will be performed with the Chen2020 dataset to enable further benchmarking of the virtual cell testing to real data provided by HVES. The following are the SMART objectives to achieve the main aim:

1. Identify the primary use cases and limitations for ECM and P2D modelling.
2. Review the different sensitivity analysis parameters objectified in previous research.
3. Access different open-source PBM programmes and discuss the limitations and ease of use of each package.
4. Review the different AI and statistical based approaches for PBM, to decide what method would be suitable for the authors level of proficiency.
5. Determine which physical based parameters should be parameterised to obtain motorsport focused performance or automotive focused performance.
6. Perform AI based modelling to understand the correlation and validate the physical cell's measurements to simulated behaviours.

1.2 Originality and Contributions

The project aims to deliver an AI method for PBM parameter optimisation for a DFN. The author will use completely open-source tools to achieve this, to ensure that no barrier to entry is in place if other researchers wish to use the method developed for the AI PBM parameter optimisation.

The choice of PETLION is to further demonstrate originality and ingenuity, while the framework of this package is clean to use, some features are yet to be fully developed compared to other more developed packages. Therefore, the author can demonstrate three key features and links that PETLION could inherit:

- Addition of more formalised drive cycle and test cycles
- Addition of Chen2020 dataset for LGM50
- Cross compatibility between PETLION and Optim.jl to integrate methods for AI and/or Statistical analysis

2 Literature review

The following literature review will pivot of four key concepts which help to conceptualise the paper.

2.1 ECM compared to P2D

An ECM use Resistor and Capacitor (RC) networks to determine the electrical behaviour, this is done by lumping RC's together and corresponding RC values to obtain the OCV and SOC performance for a given cell's chemistry. In Zhang et al work it captures and discusses a few different lumped RC models of increasing order (Zhang, Xia, Li, Cao, *et al.*, 2018), pictured in Figure 1.

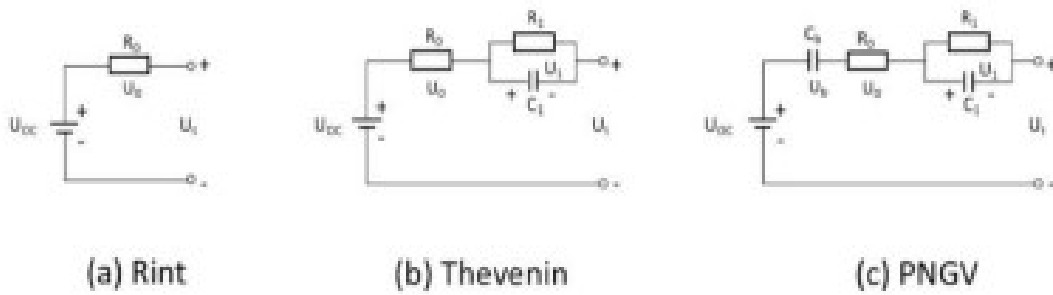


Figure 1: Commonly used battery electrical equivalent circuit models (Zhang, Xia, Li, Cao, *et al.*, 2018)

The Pseudo Two-Dimensional (P2D) Porous-Electrode model is one type of electrochemical model, which Plett covers in more depth (Plett, 2015). The fundamental of this model is that the porous material on both electrodes, is simplified to be a perfect particle in the 2D domain (Figure 2), the model then has multiple systems of PDE's that govern the behaviours such as the concentration gradients at temperature, to the mechanics of how electrons flow through the separator.

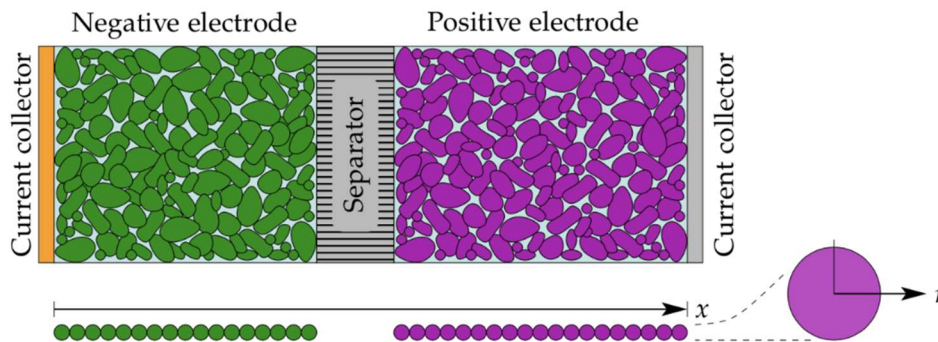


Figure 2: P2D Porous-Electrode model (Plett, 2015)

The systems of equations drive upwards of 26 different parameters, which are all defined in Bizeray et al's work (A. M. Bizeray *et al.*, 2019). This is incredibly advantageous as it gives much more control to idealise the true chemical behaviour of the cell in comparison to ECM models RC values.

In conclusion, the author has shown the fundamentals and concepts of an ECM and P2D model. The author is looking to build on how PBM are implemented but wants to emphasize the goal of the paper comes from further optimisations of the 26 parameters for PBM, as the next section (2.2) will show the challenges of measuring and validating these such parameters while A 2.1 of the appendix provides a deeper dive into the performance advantages of PBM's to ECM and other cell models (A 2.2).

2.2 Sensitivity Analysis

The importance of understanding how the 26 different parameters of a PBM perform is critical. This is done by performing a sensitivity analysis, which use sweeping changing values for a single parameter One-At-a-Time (OAT) and measures how the output changes from a fixed position. The 26 parameters are grouped into 4 sub categories in Li et al's paper (Li *et al.*, 2020):

- Geometric parameters – 11 parameters
- Transport parameters – 9 parameters
- Kinetic parameters – 3 parameters
- Concentration parameters – 3 parameters

These parameters have applied boundary conditions which then are OAT calculated, the larger majority of papers have chosen to present how terminal voltage is affected. Terminal voltage is primarily chosen as this is much easier to validate to real world data sets, however Li et al's paper does show how alternative such as SOC and capacity have different parameters sensitivities (Li *et al.*, 2020).

The highly sensitive parameters are capacity related parameters which belong primarily in the Geometric and Transport subgroups. However, the challenge becomes being able to obtain the relevant data accurately and physically for the parameters.

As shown in Figure 3, it shows a few of the methods required to obtain the parameters values for a given cell chemistry.

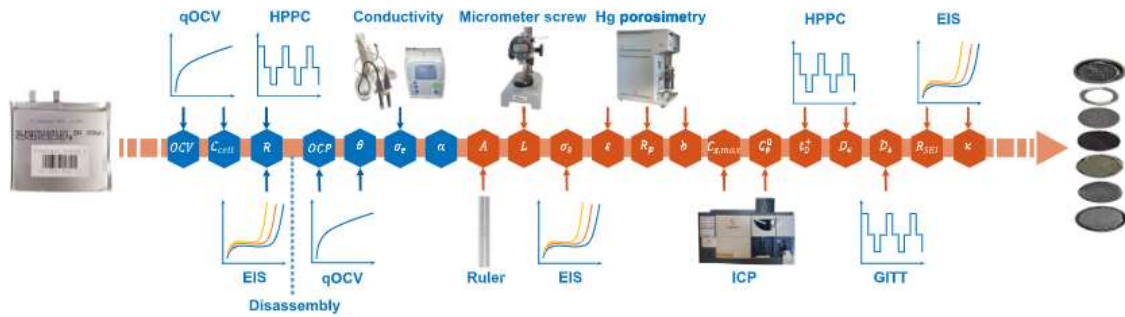


Figure 3: Schematic of experiment-based parameter identification (Li et al., 2022)

These methods require disassembly of the cell and expensive testing equipment to obtain individual and targeted values for the PBM, which even with just a single measured data point it does not depict the full model.

In conclusion, the author has shown the purpose of sensitivity analysis, outlined what is objectified in the analysis and some of the challenges of obtaining the data. In the next section (2.3) it will show the data-driven approach to populating the parameters and contained in A 2.3 of the appendix it outlines what methods have been used from literature and which are the most sensitive parameter determined by multiple authors.

2.3 Data-driven Optimisation

The need for data driven optimisations is critical, by looking to group parameter sets and validate the PBM. Li et al's further work shows this in Figure 4.

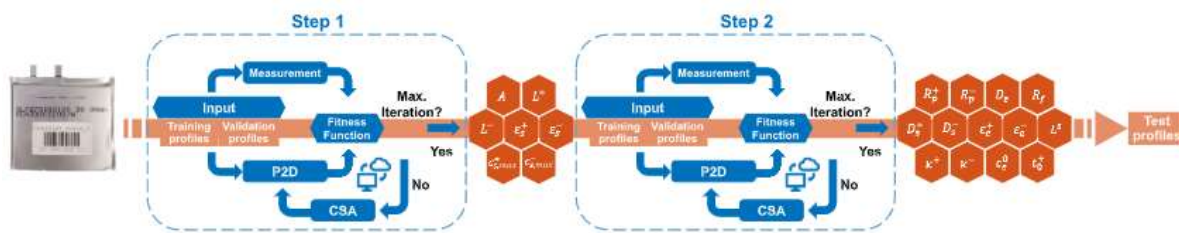


Figure 4: Schematic of the multi-objective multi-step data-driven identification process (Li et al., 2022)

By integrating machine learning techniques in a multi-stage process, it enables to populate close fitting values for a respective chemistry. The primary strategy W. Li et al's work deploys is the Cuckoo Search Algorithm (CSA) which was developed by Yang et al (X. -S. Yang and Suash Deb, 2009). The CSA is a generational based

algorithm which iteratively finds the optimal solution by replacing the worst solution in each new generation, the user defines the maximum number of iterations to avoid a never-ending loop.

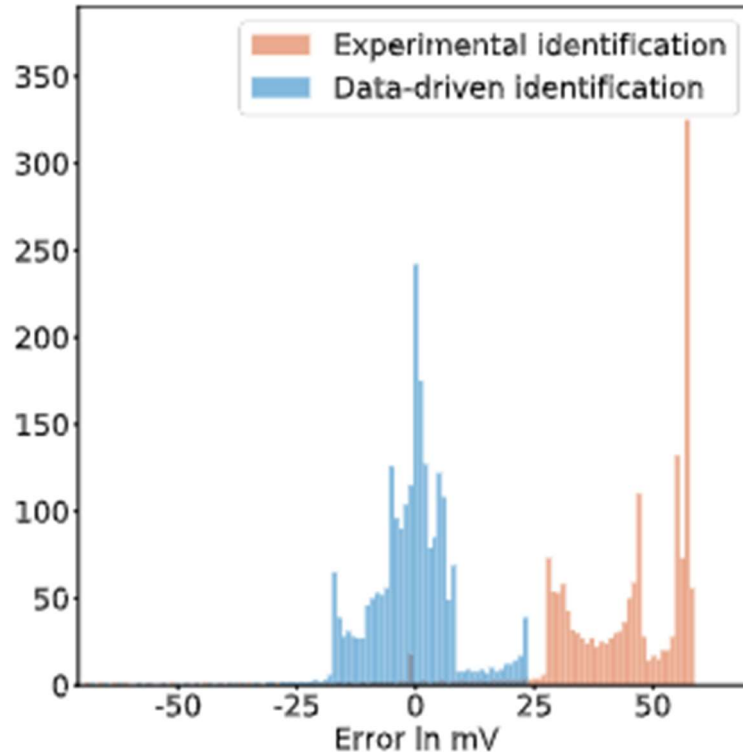


Figure 5: Error distributions of the invasive experimental and data-driven parameter identification results under 2C discharge (Li et al., 2022)

Figure 5 demonstrates clearly the performance advantage of how the CSA algorithm outperforms the experimentally populated values for a 2C discharge experiment, as the Voltage RMSE has been reduced compared to the experimental identification.

In conclusion, the author has shown one of the current approaches to populating the 26 different parameters with data-driven techniques. In the final section (2.4), the author will look at another alternative AI approach and state why the strategy is at the focus of this project.

2.4 PSO Optimisation

The final aspect of the literature review is looking at the Particle Swarm Optimization (PSO) an artificial generative model developed by Kennedy and Eberhart in 1995, which simulates the thinking pattern of a swarm of animals to determine the global minimum for an objective function (J. Kennedy and R. Eberhart, 1995).

It is strongly debated what algorithms persists as AI-focused, the author views a PSO as an AI method as it is based upon using artificial life to come to the decision of a global minimised result while tying an evolutionary element where generations feedback prior learning to inform the global best result, with no real ability for the user to iteratively intervene upon the solution. An interesting observation from Li et al's work shows the difference of performance for a PSO to the CSA method described in section 2.3, this is captured in Figure 6.

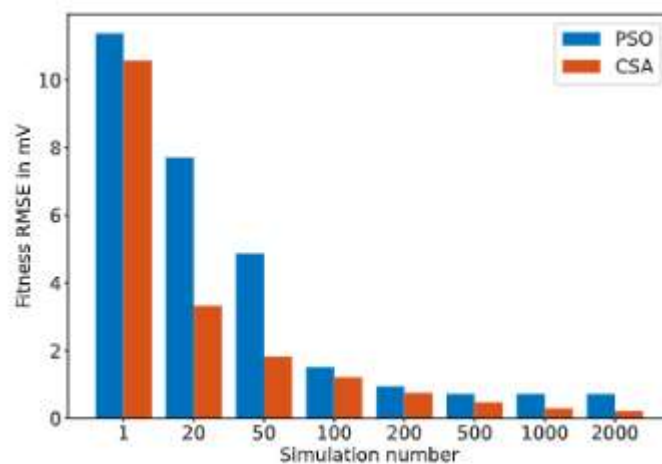


Figure 6: PSO against CSA for simulation iterations and RMSE voltage error (Li et al., 2022)

While convergence is faster in the quantity of simulation steps and the fitness is RMSE is reduced further than 200 iterations for a CSA, Li et al mentions that computational requirements and time are far greater compared to a PSO which is the primary benefit the author wishes to exploit.

In conclusion, the author has described the fundamental mechanics of the PSO and outlined the opportunity of developing this approach into a PBM and contained in the appendices (A 2.4) it elaborates further on the different optimisation techniques applied to different PBM's and performance.

3 Methodology

The overall project methodology is presented in Figure 7, where it is a 6-stage process highlighting where the objectives overlap in different colours. Boxes with a light-yellow shade indicate literature review tasks, light blue is accessing software tools and light red is the modelling phase.

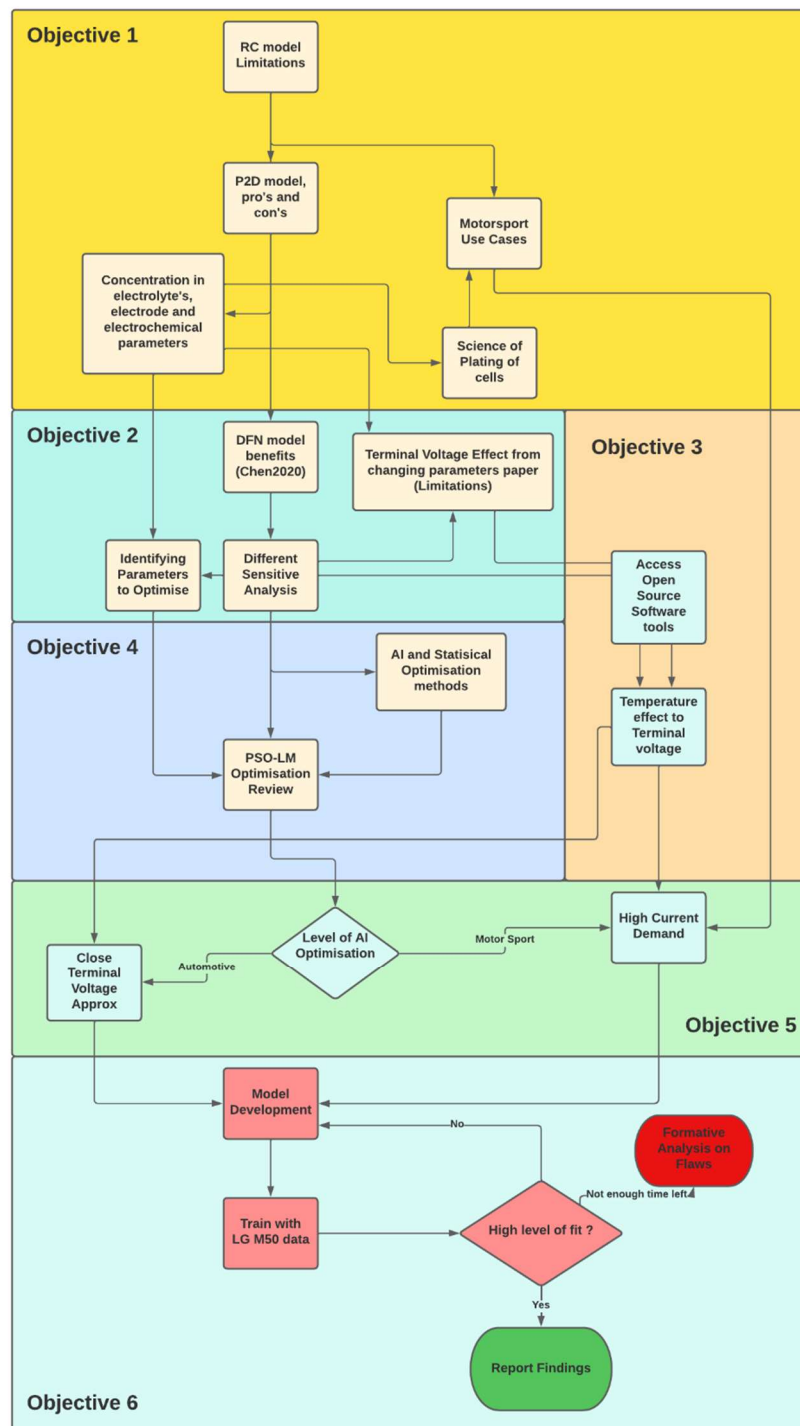


Figure 7: Overall Project Methodology

3.1 Objective 1

Primarily this objective was an initial literature review for ECM and P2D models, how they can be deployed on BMS's, and comparing the performance advantages of a P2D model with the disadvantages of hardware integration, which is covered in the initial literature review (2.1) and appendices (A 2.1).

In addition, this objective intended to look at what cell's performance characteristics are desired for both motorsport and automotive applications, in which the research into cell tab plating, concentration of electrolyte and electrode material will be discussed further in the appendices (A 2.2).

3.2 Objective 2

This objective is literature oriented, where different sensitivity analyses are reviewed. In the expectation, that the physical and chemical variables can be understood and used for Objective 5, to give what variables should be optimised for a motorsport or automotive application. Some of which is captured in the literature review before (2.2) but does not explain the limitations and assumptions needed to conduct this form of analysis.

In order for sensitivity analysis to be effective the author has to define the limits and boundaries in where sensitivity is measured, so this requires the assumption from prior experimental papers on where the boundaries must be placed (A 3.1 - Table 6). The author references boundaries outlined in Li et al's work for any of the selected parameters for OAT, as this paper extensively covers this and is the inspiration for the method the author uses (Li *et al.*, 2020).

The prime limitation of this method is doing one steady state case to indicate overall sensitivity is not sufficient, the need for different dynamic cases is needed to show how strong capacity driven parameters are with changing C-rates and DOD. The author is focusing on standardised test profiles to be emulated which will look to focus on more dynamic cases.

The method in how sensitivity is measured will be done in two ways, the first being primitive to purely see whether the simulation is working by looking at the average percentage change in the terminal voltage from a known baseline. The known baseline is computed beforehand and within the parameter sweeps will simulate the study but with the changed parameter value (A.3 - Figure 21).

The second more powerful measurement of sensitivity is Root Mean Square Error (RMSE) (1), which considers deviation from the baseline terminal voltage ($V_{baseline}$) to simulated terminal voltage (V_{sim}) with parameter change within a known sample size of data points (n).

$$RMSE = \sqrt{\sum_{i=0}^n \frac{(V_{baseline} - V_{sim})^2}{n}} \quad (1)$$

These two methods are later applied to Objective 6 and 3 to measure how terminal voltage is affected by temperature within a pure PBM simulation and the start of the framework to developing a cost function for the AI model to optimise as an output for the overriding model. In A 3.1 it outlines potential further limitations with using the Chen2020 data set for projecting terminal voltage change with temperature change and boundary conditions required for the OAT.

3.3 Objective 3

This objective is both literature oriented and software focused, where the author has accessed large databases and open-source packages, understood the benefits and withdrawals of operating in the software package/database. Summarising in A.3 - Table 5 is what the author looked at initially and what the positives and negatives are. Out of this process of researching and using these packages, two key packages were the strongest for PBM, which the author shows the features and how the software can be used to determine sensitivity with terminal voltage.

3.3.1 PyBaMM

PyBaMM is a powerful tool which has SPM, SPM_e and DFN modelling capabilities and easy to navigate features which display graphics with little effort for the author (Figure 8).

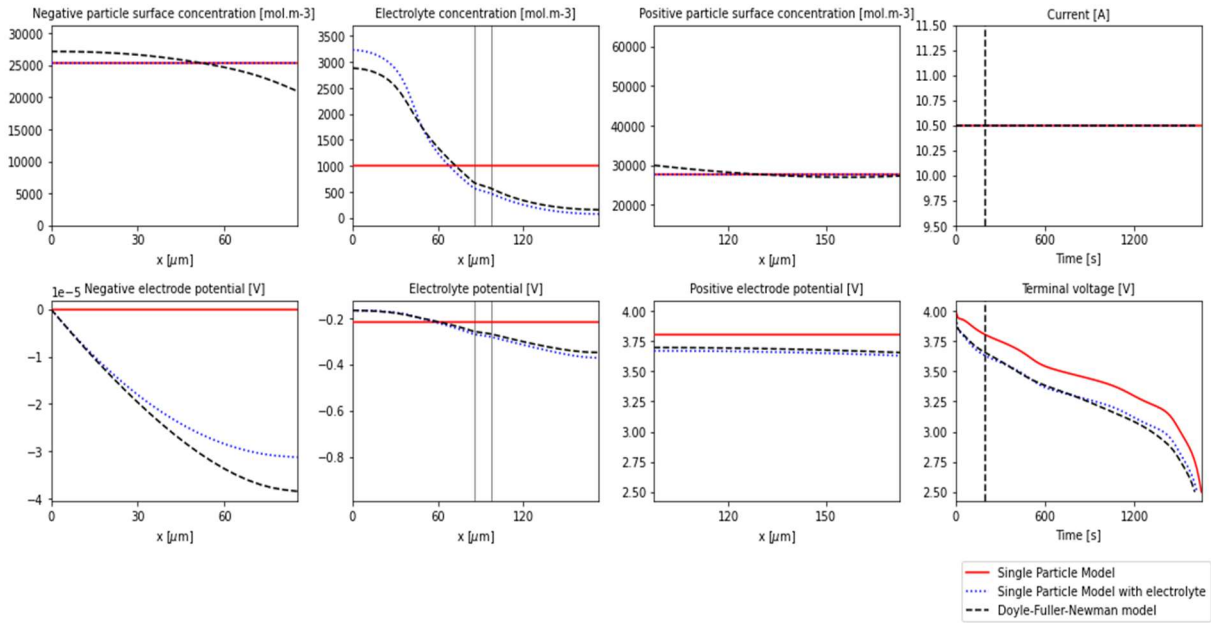


Figure 8: Chen2020 dataset simulating a 2C discharge comparing SPM, SPM_e and DFN (Planella et al., 2022)

Therefore, the author wants to incorporate these features to PETLION as outlined in A.3 - Table 5 it solves close to 22 times faster than PyBaMM, which is hugely advantageous when it comes to AI optimisations (Figure 9).

Model	Note	Evaluation Time DAE Initialization	Solver	Overhead	Total
PETLION	Symbolic Jacobian	0.110 ms	2.78 ms	0.070 ms	2.96 ms
PETLION	AD Jacobian	0.112 ms	4.39 ms	0.068 ms	4.57 ms
LIONSIMBA	Jacobian provided ^{a)}	6.51 ms	149 ms	35.3 ms	191 ms
LIONSIMBA	Jacobian on runtime	6.51 ms	149 ms	308 ms	463 ms
PyBaMM "fast"	Direct integration	65.4 ms	31.9 ms	15.4 ms	113 ms
PyBaMM "safe"	Step-and-check integration	62.4 ms	152 ms	12 ms	226 ms

a) The LIONSIMBA Jacobian cannot be reused when the parameters or variable current/power functions are modified.

Figure 9: Benchmarking of PETLION, LIONSIMBA and PyBaMM (Berliner et al., 2021)

3.3.2 PETLION

PETLION is a Julia Package which can simulate a cells behaviour using a DFN model. However, due to PETLIONS fast solving speed, the author needs to be conscious of the errors that could occur when sweeping small step sizes which could be a potential limitation. In the Appendices it shows how the Chen2020 dataset can be populated into PETLION (A 3.2)

3.4 Objective 4

This objective is literature based, where different previous research for AI and statistical based models for PBM optimisations was analysed within the initial literature review (2.3 and 2.4) and further details within the appendices of how these models function (A 2.2).

The method the author is looking create in software uses a singular objective process for optimisation, in where it performs a global search using a PSO method. Like

Objective 3 the author researched and used packages with different software environments, that could provide the foundation for the author to develop the desired method. The packages mentioned were found which could have potential to do this but state their limitations, within the appendices it outlines how the PSO is initialised (A 3.3).

3.4.1 Pyswarm

Pyswarm is a PSO gradient free method which uses Python (Pyswarm, 2022), this has been widely used and very stable to use. However, due to choosing PETLION as the main PBM package using Pyswarm via Julia would not be efficient as it would need to be rebuilt via another environment.

3.4.2 Optim.jl

Optim.jl is an Univariate and multivariate optimization tool available on Julia which includes the gradient free PSO method (Mogensen and Riseth, 2018). This performs very similarly to Pyswarm but has less examples of the package being used, so a limitation of using the package is debugging may take longer.

3.4.3 Metaheuristics.jl

Metaheuristics.jl is a global focused optimisation tool available on Julia which includes singular objective functions, multi objective focused models or many objective focused models (Mejía *et al.*, 2022). It includes a PSO method which can be used if Optim.jl is not successful as further contingency.

3.5 Objective 5

This objective is software based, where the initial groundwork for the model begins. As the author is looking to replicating previous sensitivity analysis for conditions of Chen2020. The inputs and extensive data required for the DAE's to compliment the Chen2020 dataset are contained with the appendices (A 3.2).

At the conceptualisation of the project the author was torn on what narrative the model should look to answer from the initial literature reviews, hence the decision block in the overall project methodology (Figure 7). The Author has decided to focus on the automotive approach, which looks to find close fitment to terminal voltage as there is much more literature to help support the observations the author may see. As using a current or capacity related output as a way to see variation would require a huge number of assumptions that have very little literature/journal could look to support (A.4 - Table 8).

3.6 Objective 6

The last objective is software driven. This will use the work from Objective 5 and combine it to the code for the AI based optimisation tool, furthermore this will utilise real life data generated from a full life characterisation of a LG M50 cell, to help develop the model and train the AI to yield closer fitting simulations for cell behaviour. At this stage, if the model is unsuccessful the author can formatively review the short comings of the model and approach.

The overriding methodology for how the model will integrating the features for what has been researched and built from the previous objectives (Figure 10).

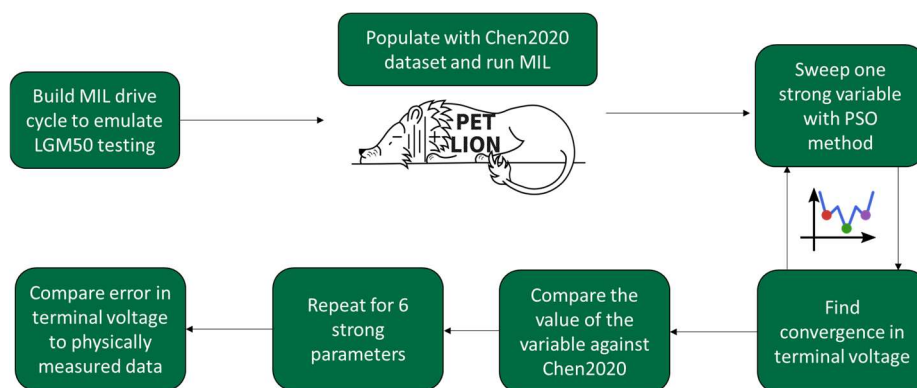


Figure 10: Overriding methodology for entire model

4 Results and Discussion

The results and discussion are separated into three sections. Section 4.1 looks to apply the methodology conceptualised in Objective 2 to demonstrate the PBM features of PETLION with temperature dependencies. While, Section 4.2 looks to go further by showing more parameters and how the package being developed is made more robust, using the methodology contained in

Objective 3 and Objective 5. Finally, section 4.3 looks to show how the PBM model has been integrated into the methodology of Objective 4 to show the final product determined by Objective 6.

4.1 Temperature sensitivity to Terminal Voltage

The author initially used the LCO dataset pre-built in PETLION to start building the code around the framework shown in Figure 21. The Author achieved this by making two functions which worked together in the main executable script, the first being the OAT function which takes an input for the desired case and inputs the boundary conditions for the nested loop. The second being the drive cycle and data plausibility checker of the nested loop, which would eliminate unreasonable results which could exceed the performance boundaries of the cell and skew how sensitive that parameter truly is.

Running the simulation for the temperature dependency with the LCO, it identified some important features to understand in the OAT approach within PETLION for advanced drive cycles (Figure 11).

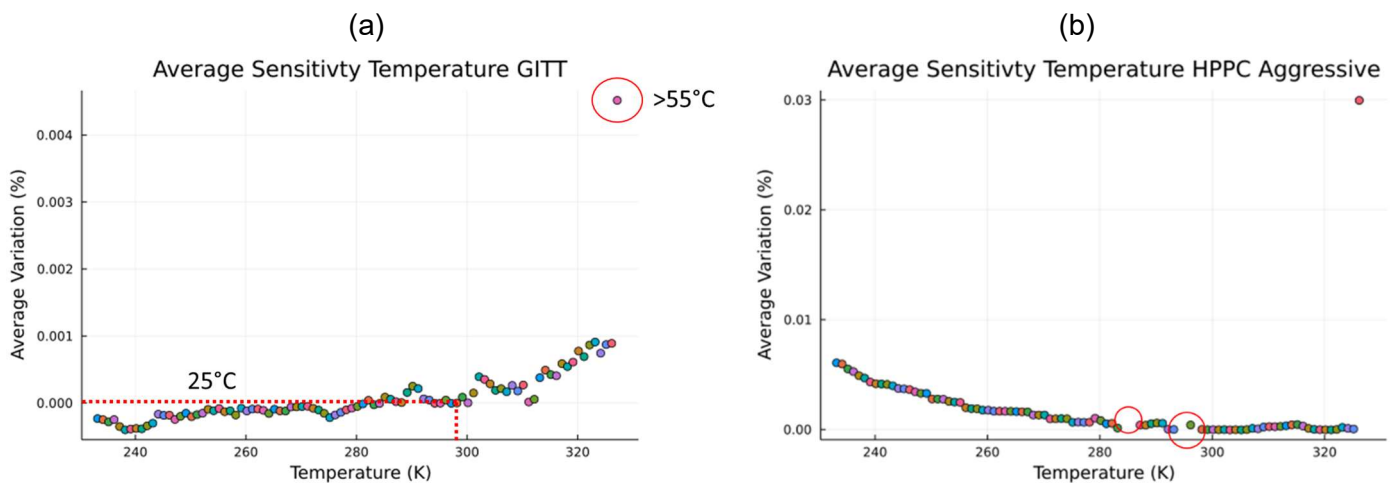


Figure 11: Average Sensitivity in Temperature for GITT (a) and HPPC (b) for LCO dataset

Figure 11a shows a large change at 323.15K (+55°C), this is due to exceeding the temperature boundaries configured for the LCO of 55°C, so at any further temperature points it outputs the same terminal voltage profile, but importantly it shows at 25°C that the average variation in terminal voltage is minimised to the original baseline simulation which is at 25°C.

Building the RMSE function (1) within Julia required some additional thought, as the main *for* loop uses Float64 values as the control iterator for OAT, however to calculate RMSE it needs to be sufficiently indexed to perform taking the mean of the delta voltage of the array with an integer value, so the addition of a *while* loop was used to help reduce constraining the main *for* loop and allow a logical statement of the RMSE index value exceeding its last index value to end the operation. Looking at the response of RMSE voltage to temperature it does correlate to the behaviours seen from thermal data (Figure 12).

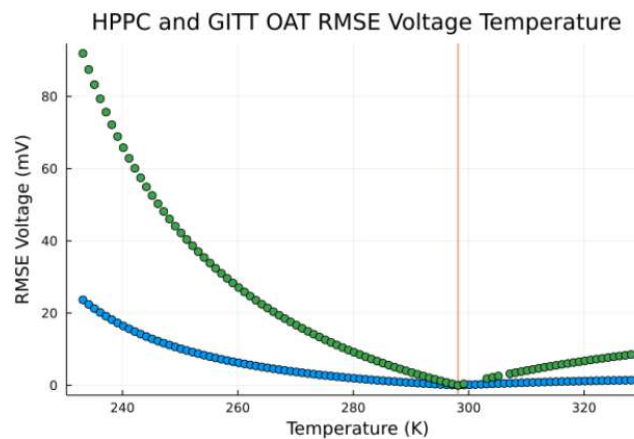


Figure 12: GITT (blue) and HPPC (green) RMSE voltage for temperature OAT with the orange line denoting benchmark temperature of 25°C for LCO

As ambient temperature decreases significantly it decreases the terminal voltage, this is more noticeable as SOC decreases. Therefore, error increases from the baseline simulation so it determines a higher RMSE value at low temperatures. The adverse happens at higher temperatures, terminal voltage looks to be increased marginally thus the error increases positively due to RMSE taking an absolute value (Figure 12a).

This is overall well supported by Zhang et al which has published the OCV and SOC curve with temperature for an Nickel Manganese Cobalt Oxide cell (Zhang, Xia, Li, Lai, *et al.*, 2018) and the general observations in terminal voltage with time on a 18650 Li-ion Cell by Wang (Wang, 2017).

4.2 Further sensitivity analysis

The author built the Chen2020 dataset within the PETLION backend by utilising the dataset in A 3.2 - Table 7 with focus on equations (5) to (9) to drive the OCV curves of the Chen2020 dataset. In Figure 13 it shows how well the terminal voltage profile of the true measured data compares the PETLION simulated result for a GITT cycle, the C-rate is well matched for both magnitude and when the pulses and rests occur.

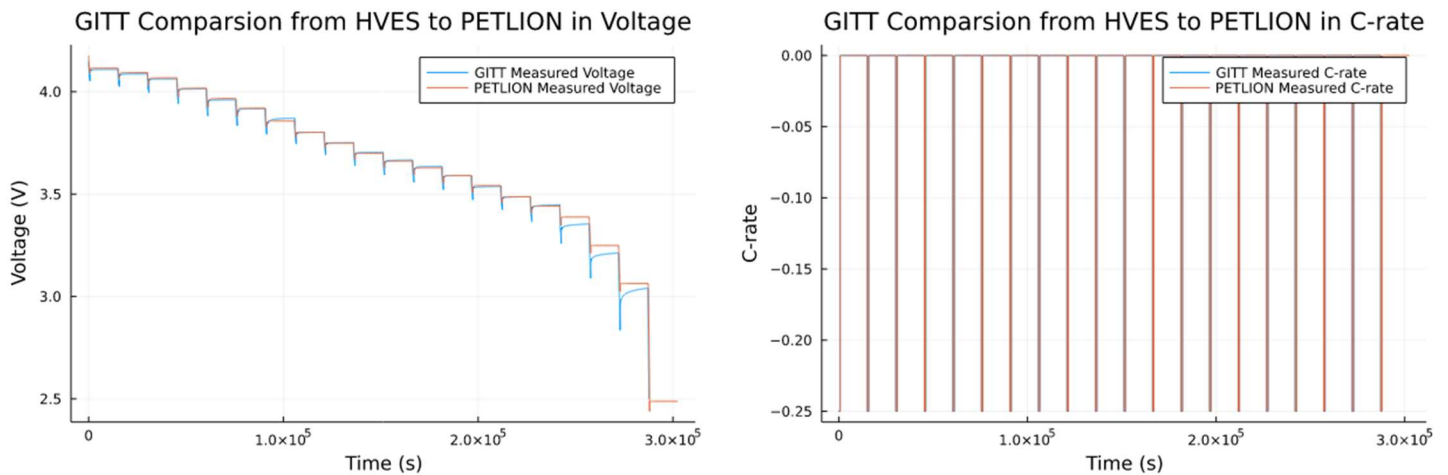


Figure 13: GITT comparison of real-world LGM50 data against PETLION simulated voltage and C-rate

The difficulty then becomes matching the data lengths and draw a correlation between the simulated response and measured response to enable the use of RMSE (1). As in the measured data for the LG M50 the array lengths are upwards of 40,000 data points, while the array length that PETLION outputs is approximately 20 times smaller at ~2,000 data points, so filtering by time must be applied to truly understand the correlation between the physical and simulated responses (Table 1).

Table 1: Correlation and RMSE of Drive cycles from PETLION to Measured Data for LGM50

Drive Cycle	Correlation in Terminal Voltage (R)	RMSE (mV)
GITT	0.995	55.8
HPPC	0.981	66.4
WLTP	0.989	16.5

In the appendices (A 6.1) it provides more graphics for HPPC (A 6.1 - Figure 22) and WLTP (A 6.1 - Figure 23), outlines the issue of indexing by timeseries in greater detail and potentially what the author could have done differently.

The Chen2020 dataset was OAT swept using a nested loop for the strongest parameters identified in A.3 - Table 6, where the GITT RMSE results are contained in Figure 14.

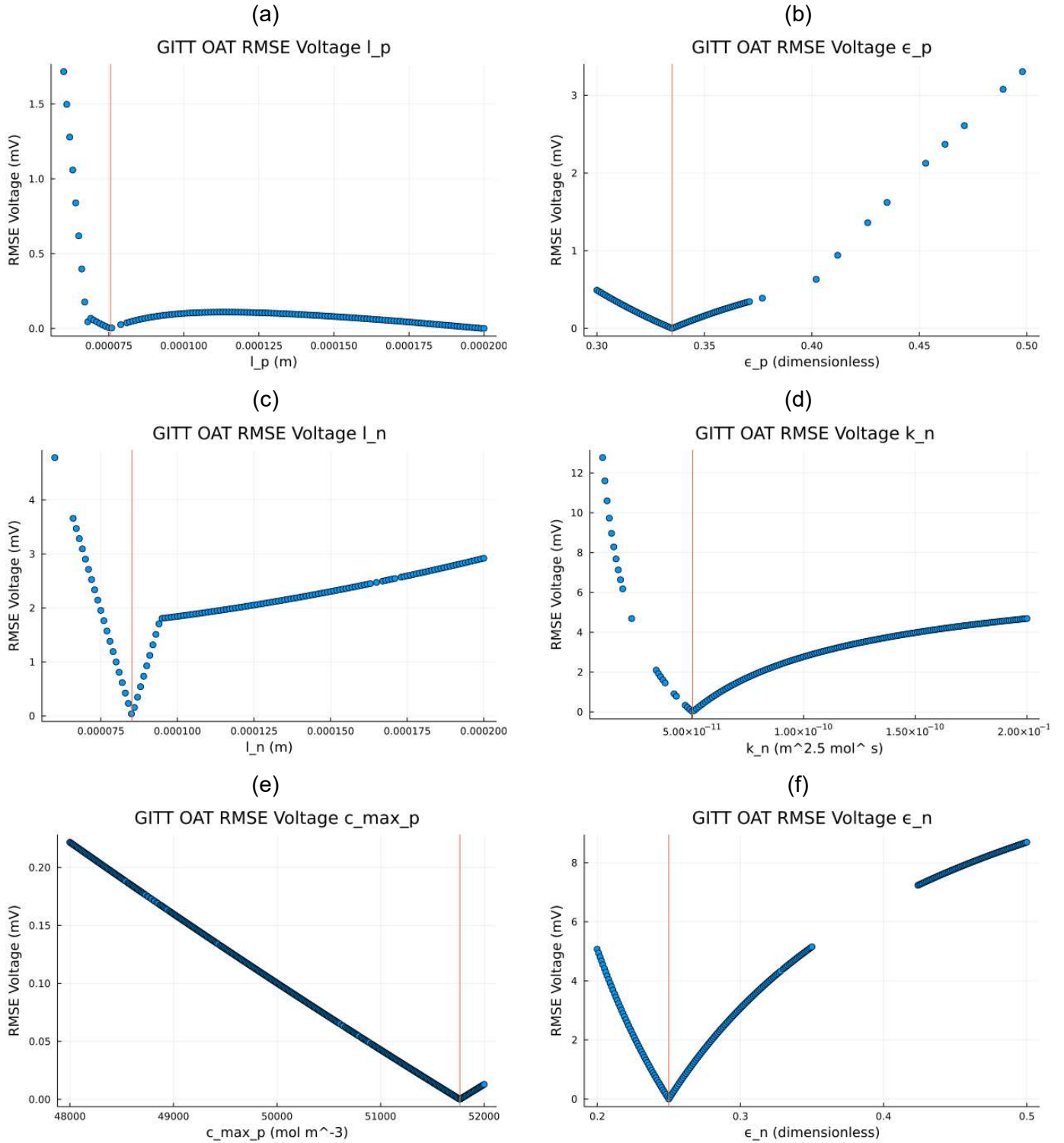


Figure 14: RMSE in Terminal voltage for I_p (a), ϵ_p (b), I_n (c), k_n (d), $c_{max,p}$ (e) and ϵ_n (f) for GITT, where the Orange line denotes the original point of the LGM50 dataset

Primarily observing and understanding a relationship of how the parameters measure against RMSE terminal voltage is excellent to see, but not critical. The critical element is to see that the simulation verifies the pre-allocated values (orange line) by observing the minimised RMSE in terminal voltage from a baseline simulation, this gives confidence to the author whatever optimisation tool is used on top of the environment built in PETLION that the objective function of RMSE can be minimised when looking in the determined boundaries.

The problem then becomes when looking at Figure 14a, the minimised RMSE occurs at more than one location within the boundary condition set for that parameter, so the AI optimisation tool will need to detect the best global minimum from one another and ensure that the authors boundary conditions are able to potentially isolate this.

Additionally seen in a large majority of Figure 14f there are regions with no points, this is primarily due to the simulation outputting a terminal voltage result which exceeds the realistic boundaries of the LGM50, as with in the drive cycle function the use of omit *NaN* is used to ensure the value could not affect any downstream code such as being used as a false optimal result. But this may become difficult for the AI method if it is close to the global best result or is stuck in a region where no points can compute through PETLION.

In order to determine the most sensitive parameter the author had produce a method that could fairly represent this statistic by accounting for the amount of data points run, so presented below is a method to drive a Sensitivity Index (SI) for the parameters OAT (2).

$$SI = \frac{\max(RMSE_{HPPC}) - \max(RMSE_{GITT})}{\text{mean}(RMSE_{GITT})} \quad (2)$$

The author recognises that this is potentially a crude method, however, it does highlight how dynamics of a test cycle can affect the terminal voltage error from the baseline dataset of Chen2020 which does ultimately show which parameter is the most sensitive, regardless of the boundary conditions used.

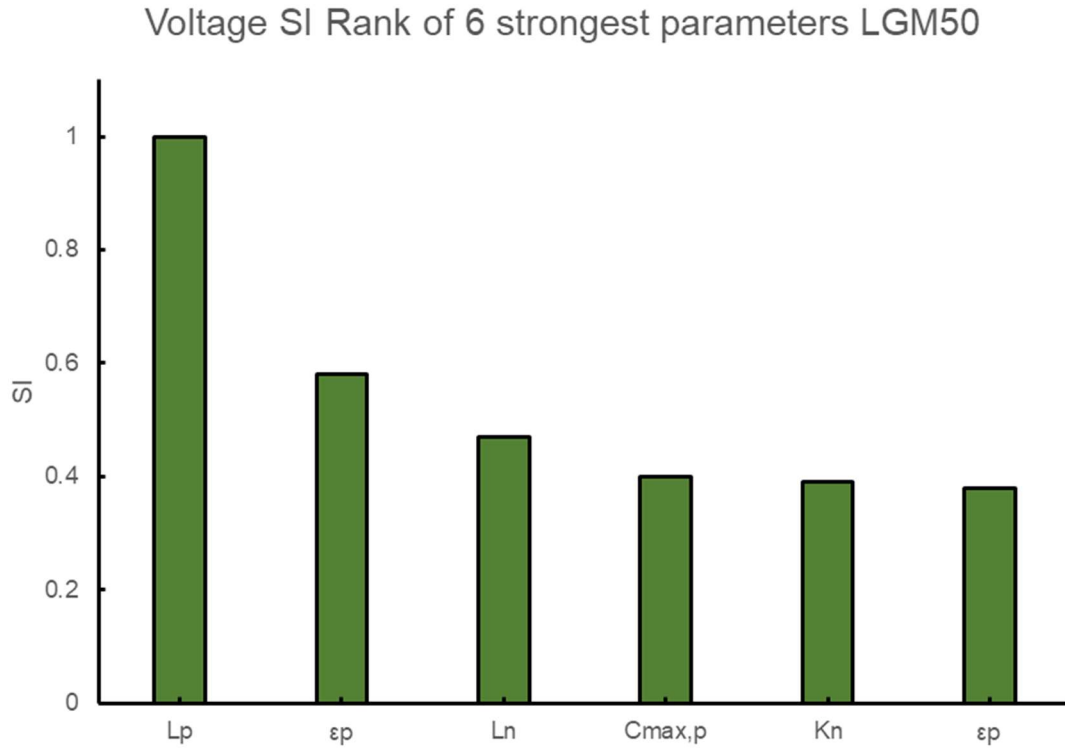


Figure 15: Ranking of Parameter Sensitivity for the LGM50 dataset within PETLION

The author considers the Cathode Thickness (L_p) to be the most impactful for change in RMSE voltage, this coincides well with Li et al's paper which uses the OAT approach for a DFN (Li *et al.*, 2020) and Gao et al's paper which uses a Monte Carlo approach for a DFN (Y. Gao *et al.*, 2021). The only parameters that are out of rank with Li et al's paper is the Cathode Maximum Ionic Concentration ($C_{p,max}$) and Anode Reaction Rate Coefficient (K_n) which should be switched round, but critically the agreement of L_p as the most impactful parameter is there.

The Author is satisfied that the method works within PETLION and if desired this could be completed with more parameters to further gauge what impact the remaining 20 parameters would have to the PETLION model created for a LGM50.

4.3 AI Optimisation

The author started building the PSO environment within Optim.jl, however it did not seem to compute a result, show that it was calling upon the built RMSE function nor provide any package level feedback into how to debug the issue. The attempted debugging by running manual breakpoints within Optim.jl uncovered that it did not like the data format of the RMSE cost function so the author reached out to the Optim.jl community to look to solve the issue, but this was not successful in finding a resolution and the author did not wish to change how the RMSE would be formatted.

However, the author looked tirelessly for another package which could be more robust and pass the RMSE cost function, and found Metaheuristics.jl which is a global focused optimisation tool that includes singular objective functions, or multi objective focused models (Mejía *et al.*, 2022). Fortunately, this package indeed was able to run the RMSE function, so the author could start progressing with the methodology laid out in Figure 10.

First the author focused on ensuring that the 20 particles initialised and finding the global best result generationally, L_p was selected initially as this is the most sensitive parameter that was addressed in Section 4.2. This was achieved by using a PETLION generated baseline of the GITT drive cycle (V_{sim}) loaded with the Chen2020 parameters to optimise ($V_{baseline}$), while the PSO is taking L_p without an initial guess (assigned as a random value) close to Chen2020's value but constrained within the parameter boundaries outlined in A 3.1 - Table 6.

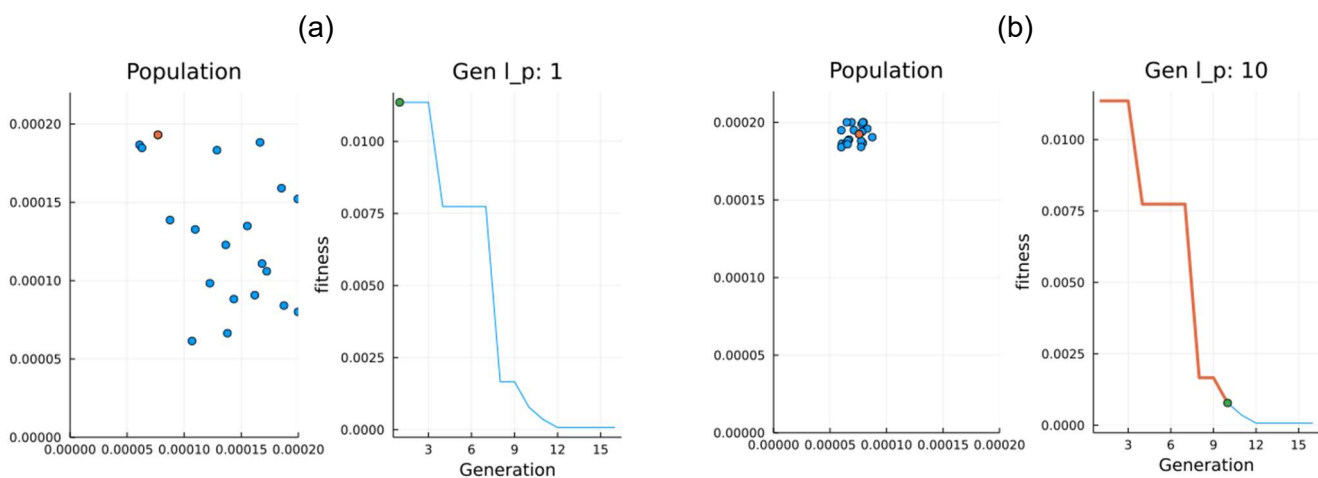


Figure 16: Global particles swarm with the fitness of the RMSE voltage at initialisation (a) and at 10th generation (b)

Figure 16 overall shows the progression and movement of the PSO, this is clearly evident at the 10th generation (Figure 16b) where the particle swarm is much closer to the global best (Orange point) compared to Figure 16a where the particle swarm has a large spread compared to the global best from the first initialisation. Now there is a high level of confidence that the PSO can minimise RMSE without an initial guess close to the Chen2020 dataset, this was repeated for all of the remaining 5 strongest parameters individually.

Table 2: PSO results for PETLION Virtual Validation for GITT

Parameter	Random Initial guess	RMSE best (V)	PSO parameter value	Percentage difference from Chen2020 (%)	Generations / Function Calls
Cathode Thickness (L_p)	$9.1 \cdot 10^{-5}$	$6.68 \cdot 10^{-10}$	$7.56 \cdot 10^{-5}$	$4.7 \cdot 10^{-7}$	272 / 5440
Cathode Porosity (ϵ_p)	0.421	$5.26 \cdot 10^{-10}$	0.335	$3 \cdot 10^{-7}$	276 / 5580
Anode Thickness (L_n)	$17 \cdot 10^{-5}$	$8.52 \cdot 10^{-5}$	$8.52 \cdot 10^{-5}$	$-4.7 \cdot 10^{-7}$	269 / 5380
Anode Reaction Rate Coefficient (K_n)	$3.0 \cdot 10^{-11}$	$6.18 \cdot 10^{-10}$	$5.03 \cdot 10^{-11}$	$-9.2 \cdot 10^{-6}$	245 / 4900
Cathode Maximum Ionic Concentration ($C_{p,max}$)	48741	$4.93 \cdot 10^{-10}$	51764	$1.4 \cdot 10^{-8}$	274 / 5480
Anode Porosity (ϵ_n)	0.37	$6.08 \cdot 10^{-10}$	0.25	$7.2 \cdot 10^{-7}$	272 / 5440

Table 2 highlights how robust this approach is due to the high fitment to the Chen2020 dataset when fed with an incorrect initial guess, while simulating purely as a virtual test cycle for GITT. Each parameter was limited to 1200 seconds for it to determine the best solution so in total this took close to 2 hours for the 6 parameters. Importantly listed in Table 2 is the function calls and generations, which is the number times the particles called the RMSE function to solve for fitness.

Now moving to the final stage of the AI optimisation process (Figure 10) is the ability to optimise the DFN parameter set when fed with physically measured data. As the prior step is comparing a simulation to another simulation it is expected there will be high fitment when the model is comparing against itself. Table 1 shows with the experimentally populated values for the Chen2020 dataset in PETLION it achieved no less than 16.5mV of RMSE, so any step to decrease this RMSE will alter the experimentally determined parameter value.

To completely ensure this method is more versatile, all 6 parameters were run together in the same objective function for a WLTP drive cycle, instead of performing an individual fitness of functions on each parameter separately and using more dynamic data such as the WLTP. This truly presents a real case when most of the critical PBM parameters for a cell are not understood, the summary results are contained in Table 3 which was limited to 3600s at an average of 8 seconds per function call.

Table 3: PETLION PSO results for measure data WLTP

Parameter	Random Initial guess	RMSE best (mV)	PSO parameter value	Percentage difference from Chen2020 (%)
Cathode Thickness (L_p)	$9.1 \cdot 10^{-5}$	9.78	$8.05 \cdot 10^{-5}$	-6.54
Cathode Porosity (ϵ_p)	0.421		0.3	10.4
Anode Thickness (L_n)	$17 \cdot 10^{-5}$		$10 \cdot 10^{-5}$	-17.4
Anode Reaction Rate Coefficient (K_n)	$3.0 \cdot 10^{-11}$		$2.5 \cdot 10^{-11}$	-50.3
Cathode Maximum Ionic Concentration ($C_{p,max}$)	48741		52000	-0.45
Anode Porosity (ϵ_n)	0.37		0.2	20

This improved the fitment of Voltage by 38% from the benchmark established from Table 1 for a WLTP with the experimentally determined dataset. However, it is important to comment on the changes of parameter values with the largest being K_n at 50.3% (Table 3). This is due to the anode reaction rate coefficient understood from Chen2020 dataset not been correctly input into PETLION due to using a different unit. The voltage profile for the PSO generated WLTP is found in Figure 17, which highlights the better capture of dynamics when compared to the initial experimentally parameter driven simulation (A 6.1 - Figure 23).

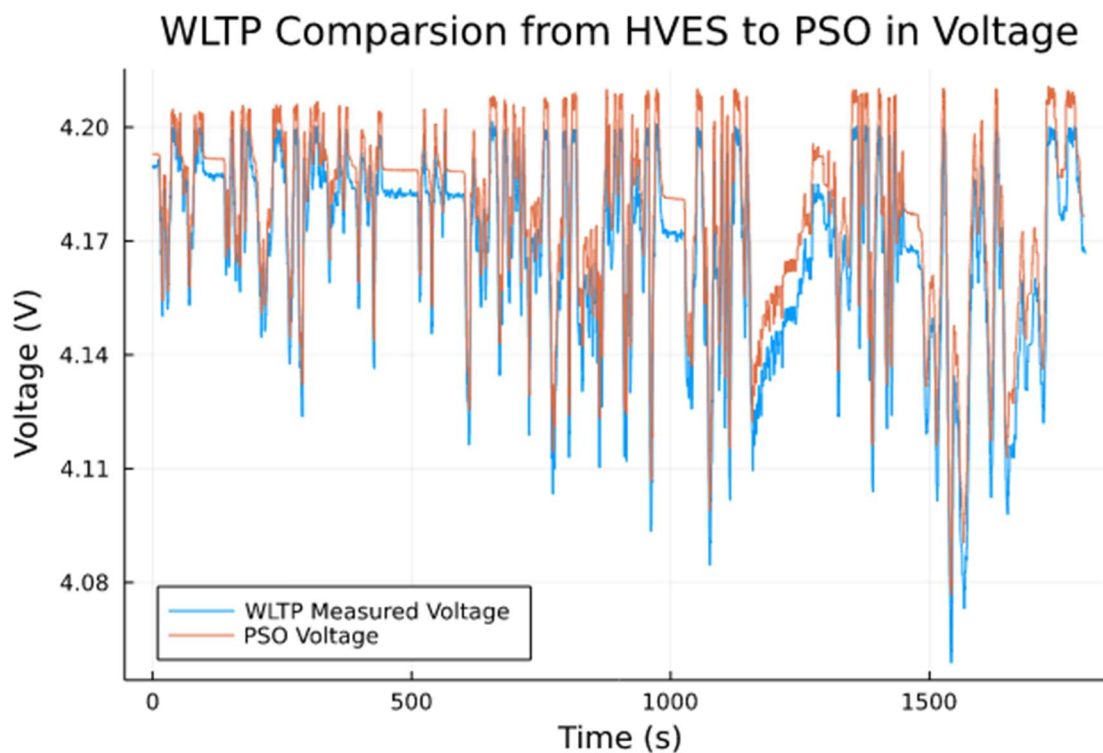


Figure 17: WLTP response driven by PSO optimization

To provide further validation this was repeated for a GITT drive cycle and is contained in the appendices (A 6.3) which follows the same conclusions presented for the WLTP.

5 Conclusions

The author has clearly outlined and delivered upon all of the objectives contained in the whole project methodology (Figure 7) to achieve in developing an Artificially Informed Data Driven Physics Based Battery Model Parameterisation with a PSO method for the LG M50 dataset. This was achieved by extensively reviewing close to 30 papers published on topics such as PBM, AI modelling and Sensitivity analysis. With all battery focused content being within the previous 7 years and including 12 papers that have been published in 2022. This truly highlights the advanced nature of this field of research in PBM optimisation with AI methods, with fresh literature to help inform and back up the results of this thesis.

The PETLION environment built achieved a high level of correlation and marginal error in terminal voltage response for multiple different test and drive cycles (Table 1) for the Chen2020 data set. In addition to this the OAT approach developed in tandem with PETLION clearly showed the versatility of using Voltage RMSE as an objective function (Figure 14) to determine a minimised result for all of the 6 strongest parameters indicated from literature (A 2.3). Using the ranking system developed by the author (2) to determine the sensitivity index for all 6 parameters (Figure 15) for both HPPC and GITT cases aligns well with the observations seen in the literature covered (A 2.3).

The PSO method built within the PETLION environment produced excellent fitness to the singular objective function of terminal voltage when purely training with virtually generated data (Figure 16) and additionally showed how robust the approach is when the initial guess is a random starting point contained within a realistic boundary for the parameter (Table 2).

The final stage of the PSO validation methodology (Figure 10) was then applied to real measured data to verify that this model can accurately determine the parameters. This did encounter problems with how the input of measured data is presented to the objective function, however it was able to minimise the RMSE voltage by 38% for a WLTP (Table 3) providing a better fit for terminal voltage for the LGM50, which is a huge success from the authors perspective.

Computationally this was able to complete a WLTP function call every 8 seconds, with 300 seconds of pre-allocation for the PETLION Jacobian PBM model, so in total to achieve a RMSE of 9.78mV it takes under 1.5 hours to simulate completely. Which is ~10 times faster than Li et al's CSA approach on a system which has 26 cores, against the author which has not utilised multi-threading and achieves a similar result for minimised voltage RMSE with less data (Li *et al.*, 2022).

However, not every aspect of this thesis was successful, from the initial concept of being able to use Optim.jl it was not possible due to having software integration problems but was mitigated by changing to Metaheuristics.jl. The conditioning and matching of time series data provided a higher RMSE error than expected (Table 1), so using an alternative technique such as Dynamic Time Warping could potentially solve this issue and make model input more robust (Müller, 2007).

The author wants to highlight the choice of dataset, Chen2020 is not perfect, but it is the currently the most invasive experimental paper for the LGM50, in the appendices (A 3.1) it outlines the limitations which Chen et al recognises (Chen *et al.*, 2020). Therefore, in the ageing of this thesis there potentially may be another data set for the LGM50 which may improve on the parameter driven OCV fitment, which will help data-driven algorithms in the future to target further fitness in OCV.

Reflecting on the work displayed, the author has areas of interest within the thesis that could be explored more deeply post submission. The first being contained in section 4.2 where only 6 parameters were used, the author wishes to perform the OAT on all 26 parameters to truly see if the observations captured in A 2.3 match for terminal voltage sensitivity among different papers. The second being the further inclusion of the 26 parameters into the PSO optimisation (4.3) to see the impact of solving time and understanding the performance benefit of multi-threading when compared to Fan et al's work which performs a PSO DFN optimisation (Fan, 2020).

In conclusion, the author is delighted that a completely unique PBM AI optimisation toolbox which outputs high fitting terminal voltage responses for an LGM50 has been produced, and subsequently will release this project toolbox on GitHub for the submission of the thesis.

6 References

- A. M. Bizeray *et al.* (2019) 'Identifiability and Parameter Estimation of the Single Particle Lithium-Ion Battery Model', *IEEE Transactions on Control Systems Technology*, 27(5), pp. 1862–1877. Available at: <https://doi.org/10.1109/TCST.2018.2838097>.
- Andersson, M. *et al.* (2022) 'Parametrization of physics-based battery models from input–output data: A review of methodology and current research', *Journal of Power Sources*, 521, p. 230859. Available at: <https://doi.org/10.1016/j.jpowsour.2021.230859>.
- Berliner, M.D. *et al.* (2021) 'Methods—PETLION: Open-Source Software for Millisecond-Scale Porous Electrode Theory-Based Lithium-Ion Battery Simulations', *Journal of The Electrochemical Society*, 168(9), p. 090504.
- Bezanson, J. *et al.* (2017) 'Julia: A fresh approach to numerical computing', *SIAM Review*, 59(1), pp. 65–98. Available at: <https://doi.org/10.1137/141000671>.
- Chen, C.-H. *et al.* (2020) 'Development of Experimental Techniques for Parameterization of Multi-scale Lithium-ion Battery Models', *Journal of The Electrochemical Society*, 167(8), p. 080534. Available at: <https://doi.org/10.1149/1945-7111/ab9050>.
- Doyle, M., Fuller, T.F. and Newman, J. (1993) 'Modeling of Galvanostatic Charge and Discharge of the Lithium/Polymer/Insertion Cell', *Journal of The Electrochemical Society*, 140(6), pp. 1526–1533. Available at: <https://doi.org/10.1149/1.2221597>.
- Fan, G. (2020) 'Systematic parameter identification of a control-oriented electrochemical battery model and its application for state of charge estimation at various operating conditions', *Journal of Power Sources*, 470, p. 228153. Available at: <https://doi.org/10.1016/j.jpowsour.2020.228153>.
- G. Florentino and M. S Trimboli (2018) 'Lithium-ion Battery Management Using Physics-based Model Predictive Control and DC-DC Converters', in *2018 IEEE Transportation Electrification Conference and Expo (ITEC). 2018 IEEE Transportation Electrification Conference and Expo (ITEC)*, pp. 916–921. Available at: <https://doi.org/10.1109/ITEC.2018.8450187>.
- Hwang, G. *et al.* (2022) 'Model predictive control of Lithium-ion batteries: Development of optimal charging profile for reduced intracycle capacity fade using an enhanced single particle model (SPM) with first-principled chemical/mechanical degradation mechanisms', *Chemical Engineering Journal*, 435, p. 134768. Available at: <https://doi.org/10.1016/j.cej.2022.134768>.
- J. Kennedy and R. Eberhart (1995) 'Particle swarm optimization', in *Proceedings of ICNN'95 - International Conference on Neural Networks. Proceedings of ICNN'95 - International Conference on Neural Networks*, pp. 1942–1948 vol.4. Available at: <https://doi.org/10.1109/ICNN.1995.488968>.
- Li, W. *et al.* (2020) 'Parameter sensitivity analysis of electrochemical model-based battery management systems for lithium-ion batteries', *Applied Energy*, 269. Available at: <https://doi.org/10.1016/j.apenergy.2020.115104>.
- Li, W. *et al.* (2022) 'Data-driven systematic parameter identification of an electrochemical model for lithium-ion batteries with artificial intelligence', *Energy Storage Materials*, 44, pp. 557–570. Available at: <https://doi.org/10.1016/j.ensm.2021.10.023>.

Liu, Y. *et al.* (2020) 'Simulation and parameter identification based on electrochemical-thermal coupling model of power lithium ion-battery', *Journal of Alloys and Compounds*, 844, p. 156003. Available at: <https://doi.org/10.1016/j.jallcom.2020.156003>.

Lombardo, T. *et al.* (2022) 'The ARTISTIC Online Calculator: Exploring the Impact of Lithium-Ion Battery Electrode Manufacturing Parameters Interactively Through Your Browser', *Batteries & Supercaps*, n/a(n/a), p. e202100324. Available at: <https://doi.org/10.1002/batt.202100324>.

Mehta, A. (2022) *Battery boom time*, *Chemistry World*. Available at: <https://www.chemistryworld.com/news/battery-boom-time/4015234.article> (Accessed: 8 November 2022).

Mejía, J. *et al.* (2022) 'jmejia8/Metaheuristics.jl: v3.2.11'. Zenodo. Available at: <https://doi.org/10.5281/zenodo.7051496>.

Mogensen, P.K. and Riseth, A.N. (2018) 'Optim: A mathematical optimization package for Julia', *Journal of Open Source Software*, 3(24), p. 615. Available at: <https://doi.org/10.21105/joss.00615>.

Müller, M. (ed.) (2007) 'Dynamic Time Warping', in *Information Retrieval for Music and Motion*. Berlin, Heidelberg: Springer Berlin Heidelberg, pp. 69–84. Available at: https://doi.org/10.1007/978-3-540-74048-3_4.

O'Regan, K. *et al.* (2022) 'Thermal-electrochemical parameters of a high energy lithium-ion cylindrical battery', *Electrochimica Acta*, 425, p. 140700. Available at: <https://doi.org/10.1016/j.electacta.2022.140700>.

Planella, F.B. *et al.* (2022) 'A continuum of physics-based lithium-ion battery models reviewed', *Progress in Energy*, 4(4), p. 042003. Available at: <https://doi.org/10.1088/2516-1083/ac7d31>.

Plett, G.L., , (2015) *Battery management systems. Volume I, Volume I.*. Available at: <https://app.knovel.com/hotlink/toc/id:kpBMSVBM02/battery-management-systems/battery-management-systems>.

Pyswarm, (2022) 'Pyswarm PSO'. Available at: <https://pythonhosted.org/pyswarm/>.

Rahman, M., Anwar, S. and Izadian, A. (2016) 'Electrochemical model parameter identification of a lithium-ion battery using particle swarm optimization method', *Journal of Power Sources*, 307, pp. 86–97. Available at: <https://doi.org/10.1016/j.jpowsour.2015.12.083>.

Santhanagopalan, S., Guo, Q. and White, R.E. (2007) 'Parameter Estimation and Model Discrimination for a Lithium-Ion Cell', *Journal of The Electrochemical Society*, 154(3), p. A198. Available at: <https://doi.org/10.1149/1.2422896>.

Shen, W.-J. and Li, H.-X. (2017) 'Multi-Scale Parameter Identification of Lithium-Ion Battery Electric Models Using a PSO-LM Algorithm', *Energies*, 10(4). Available at: <https://doi.org/10.3390/en10040432>.

Sulzer, V. *et al.* (2021) 'Python Battery Mathematical Modelling (PyBaMM)', *Journal of Open Research Software*, 9(1), p. 14. Available at: <https://doi.org/10.5334/jors.309>.

Synopsys (2022) 'What is a Battery Management System (BMS)? ♦ How it Works | Synopsys', *Synopsys.com*. Available at: <https://www.synopsys.com/glossary/what-is-a-battery-management-system.html>.

Torchio, M. *et al.* (2016) 'LIONSIMBA: A Matlab Framework Based on a Finite Volume Model Suitable for Li-Ion Battery Design, Simulation, and Control', *Journal of The Electrochemical Society*, 163(7), pp. A1192–A1205. Available at: <https://doi.org/10.1149/2.0291607jes>.

Vazquez-Arenas, J. *et al.* (2014) 'A rapid estimation and sensitivity analysis of parameters describing the behavior of commercial Li-ion batteries including thermal analysis', *Energy Conversion and Management*, 87, pp. 472–482. Available at: <https://doi.org/10.1016/j.enconman.2014.06.076>.

Wang, K. (2017) 'Study on Low Temperature Performance of Li Ion Battery', 4, pp. 1–12. Available at: <https://doi.org/10.4236/oalib.1104036>.

X. -S. Yang and Suash Deb (2009) 'Cuckoo Search via Lévy flights', in *2009 World Congress on Nature & Biologically Inspired Computing (NaBIC)*. *2009 World Congress on Nature & Biologically Inspired Computing (NaBIC)*, pp. 210–214. Available at: <https://doi.org/10.1109/NABIC.2009.5393690>.

Y. Bi and S. -Y. Choe (2018) 'Automatic Estimation of Parameters of a Reduced Order Electrochemical Model for Lithium-Ion Batteries at the Beginning-of-Life', in *2018 IEEE Vehicle Power and Propulsion Conference (VPPC)*. *2018 IEEE Vehicle Power and Propulsion Conference (VPPC)*, pp. 1–6. Available at: <https://doi.org/10.1109/VPPC.2018.8604954>.

Y. Gao *et al.* (2021) 'Global Parameter Sensitivity Analysis of Electrochemical Model for Lithium-Ion Batteries Considering Aging', *IEEE/ASME Transactions on Mechatronics*, 26(3), pp. 1283–1294. Available at: <https://doi.org/10.1109/TMECH.2021.3067923>.

Zhang, L. *et al.* (2017) 'Comparative Research on RC Equivalent Circuit Models for Lithium-Ion Batteries of Electric Vehicles', *Applied Sciences*, 7, p. 1002. Available at: <https://doi.org/10.3390/app7101002>.

Zhang, R., Xia, B., Li, B., Cao, L., *et al.* (2018) 'State of the Art of Lithium-Ion Battery SOC Estimation for Electrical Vehicles', *Energies*, 11, p. 1820. Available at: <https://doi.org/10.3390/en11071820>.

Zhang, R., Xia, B., Li, B., Lai, Y., *et al.* (2018) 'Study on the Characteristics of a High Capacity Nickel Manganese Cobalt Oxide (NMC) Lithium-Ion Battery—An Experimental Investigation', *Energies*, 11, p. 2275. Available at: <https://doi.org/10.3390/en11092275>.

A.1 Detailed background

The use of software packages such as MATLAB and Python are popular within academia and industry, but it does not offer the fastest execution of looped commands and has financial barriers for using the advanced optimisation features of MATLAB. This is why Julia was created to enhance performance by using Just-In-Time Compilation of code which is fast like compiling C-code, is completely open-source and its ideal use case is for data science and machine learning (Bezanson *et al.*, 2017). Additionally, the syntax and package management is user friendly to navigate in comparison to Python from the authors perspective.

The primary advantages to developing a PBM optimisation toolbox is to reduce the dependency of needing experimentally obtained values to drive a PBM, as only needing to perform the minimal test cycles which are required for battery pack development and characterisation ensures that cost and time is kept to a minimum. Pictured in Figure 3 it shows the long process of testing and obtaining parameter values at the half cell level, and this is proven by reviewing the Chen2020 dataset which demonstrates that the experimental and statistical methods used to observe parameters only achieves medium levels of OCV fitment of 46mV RMSE for a C/2 experiment when applied to a DFN model (Chen *et al.*, 2020).

When compared to the levels of fitment for an data-driven DFN model pictured in Figure 4, this approach can achieve close to ~10mV RMSE for test cycles such as a WLTP. Which is only fed an Over Potentials and electrolyte concentration conditions, which is a reduce amount of testing resource compared to fulfilling the stages seen in Figure 3 (Li *et al.*, 2022). This is the reason why the author wanted to focus on developing this thesis, to use the powerful tools of data science and AI optimisations to look to reduce the dependency of experimentally obtained values.

Summarising, the primary objective of this thesis is to research and develop Artificially Informed Data Driven Physics Based Battery Model Parameterisation with a PSO method for the LG M50 dataset.

A.2 Detailed literature review

This section looks to continue the literature review and provides more detail on the advantages to PBM modelling (A 2.1), what PBM methods are available (A 2.2), the different forms of sensitivity analysis (A 2.3) and prior optimisation methods have been used for PBM's (A 2.4).

A 2.1 Advantages of PBM modelling

This can be seen more prominently when looking at how the models are deployed onto a simulated BMS. From Trimboli's and Florentino's work from the University of Colorado (G. Florentino and M. S Trimboli, 2018) shows by deploying Model Predictive Control (MPC) measures to both PBM and ECM models that the performance benefit for PBM is significant (Figure 18).

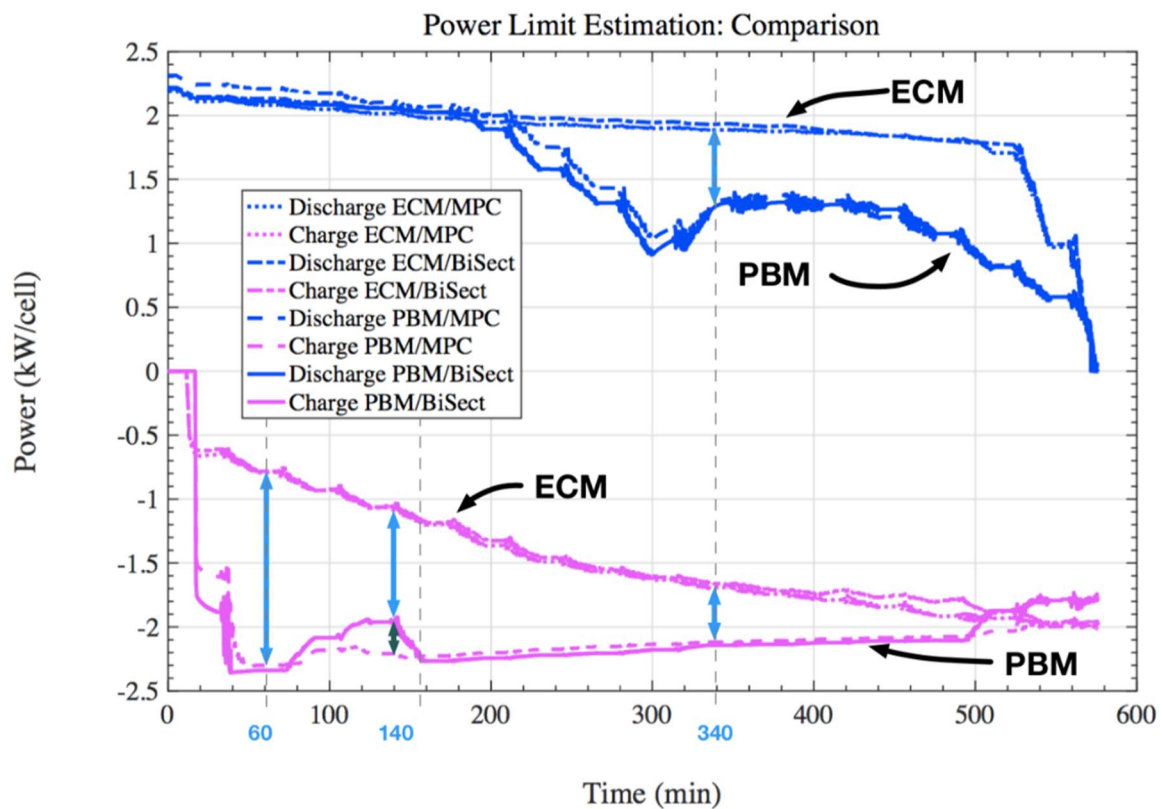


Figure 18: ECM against a PBM from MPC analysis (G. Florentino and M. S Trimboli, 2018)

Figure 18 shows an ECM over-projecting discharge performance, which will cause faster degradation for individual cells and ECM under-projects the true performance in charging.

However, this particular MPC is not that deployable to hardware BMS's as computational time is significant, which L. Zhang et al states in their conclusion for ECM models against PBM, that the computational time for a PBM is upwards of "9600 seconds" versus a "negligible amount of time" for ECM models (Zhang *et al.*, 2017).

But there is further work being produced by Hwang et al which has implemented an SPM model as an MPC to utilise the degradation mechanics of capacity fade and provide better SOC prediction compared to an ECM (Hwang *et al.*, 2022), which was tested in a closed loop environment and was able to form these update calculation for capacity degradation within 45 seconds which is significantly faster than what Zhang et al had observed in 2017.


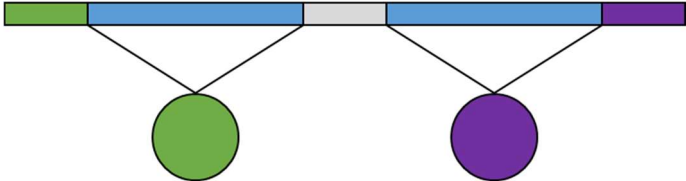
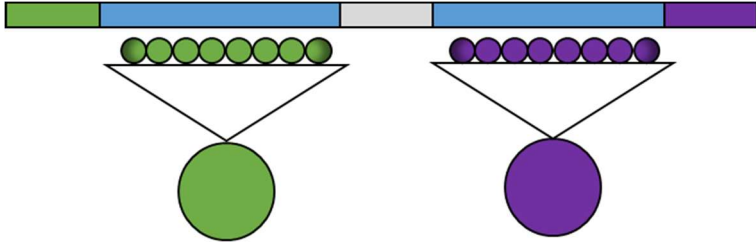
This highlights the ability of using a PBM as a background solver on a BMS to gauge further information for complex mechanics such as SEI growth, Lithium Plating and Anode Poisoning which help project the SOH for a cell, which is explained at greater length in Plett's textbook on Battery Modelling (Plett, 2015). As an ECM cannot predict SOH, SOP and degradation due to using parameters closely related to electrical components (RC values) which are not the chemical and physical parameters focused to deliver the approximations accurately.

In the next section (A 2.2) it provides information on three common PBM's used and goes into greater detail on the DFN model.

A 2.2 More PBM methods

PBM's come in many forms in varying levels of complexity, a journal compose by Planella et al provides an excellent insight into what model is appropriate to the use case, how the models are derived and overlap with one another (Planella *et al.*, 2022). Comprised in Table 4 is an overview of an SPM, SPMe and DFN.

Table 4: Comparison of 2D PBM methods

Model	General Concept	Positives	Negatives
SPM	<p>The Single Particle Model (SPM), looks solely at the interaction between the positive and negative electrode, neglecting any electrolyte dynamics.</p> 	<ul style="list-style-type: none"> • Robust and simplest model of three ideas of: <ul style="list-style-type: none"> ○ Lithium transportation ○ Thermodynamic relationship of lithium concentration and electrode potential ○ Overpotential required • Smallest number of parameters required (17) • Widely used and has been built on a BMS (Hwang <i>et al.</i>, 2022) 	<ul style="list-style-type: none"> • Does not perform well in very high dynamic events • Does not capture the true effects of the electrolyte which helps inform more advanced ageing models • Does not include ohmic losses or concentration overpotentials for the electrodes or electrolyte
SPMe	<p>The Single Particle Model with Electrolyte dynamics (SPMe), it performs like an SPM but with more equations for electrolyte and separator mechanisms.</p> 	<ul style="list-style-type: none"> • Robust and moderately simple model when compared to a DFN • Has a good fitment to a DFN when looking at terminal voltage (Figure 8) • Has potential at been built as a more advanced MPC for a BMS. 	<ul style="list-style-type: none"> • Does not perform well in very high dynamic events • 26 parameters required to drive DAE's, which is more than a SPM • Does not capture the spatial variations across the electrode
DFN (P2D)	<p>The Doyle-Fuller-Newton (DFN) or also known as P2D, builds upon the SPM with its electrolyte dynamics but introduces more perfectly round particles which is getting closer to the true microstructure of a cell.</p> 	<ul style="list-style-type: none"> • Computationally affordable when compared to running microstructure focused models • A DFN performs very well in high dynamic problems, so best utilised for drive cycle correlations to measured data • Has potential at been built as a more advanced MPC for a BMS, in comparison to a microstructure focused model 	<ul style="list-style-type: none"> • The most complex non microstructure focused model. • 26 parameters required to drive DAE's, which is more than a SPM • Still only considers the cell in two-dimensions, which there are other microstructure focused models which capture the behaviour in 3D (Homogenised model)

Diving deeper into the mechanics of the DFN model, it is formalised and bounded by the dimensions of the electrodes, separator and particle size. Complementing these physical boundaries of the DFN model, is 5 key aspects that allow the terminal voltage to be characterised by stating the PDAE's and boundaries that drive each aspect, these equations which simplified from the original paper produced by Doyle, Fuller and Newman (Doyle, Fuller and Newman, 1993).

- Electrode mass transport
- Electrolyte mass transport
- Solid potential of particles
- Electrolyte potential
- Butler-Volmer Equation

A 2.3 Sensitivity Analysis

An extensive review by Andersson et al displays the different forms of sensitivity analysis conducted for different PBM's. The journal selected and observed 5 different papers to visually compare how these papers concluded the most sensitive parameters (Figure 19).

- DFN – Local – OAT (Li *et al.*, 2020)
- DFN + Thermal – Local –OAT (Liu *et al.*, 2020)
- DFN – Global – Monte Carlo + Partial Correlation (Y. Gao *et al.*, 2021)
- DFN + Thermal – Local – OAT (Vazquez-Arenas *et al.*, 2014)
- DFN – Local –OAT (Y. Bi and S. -Y. Choe, 2018)

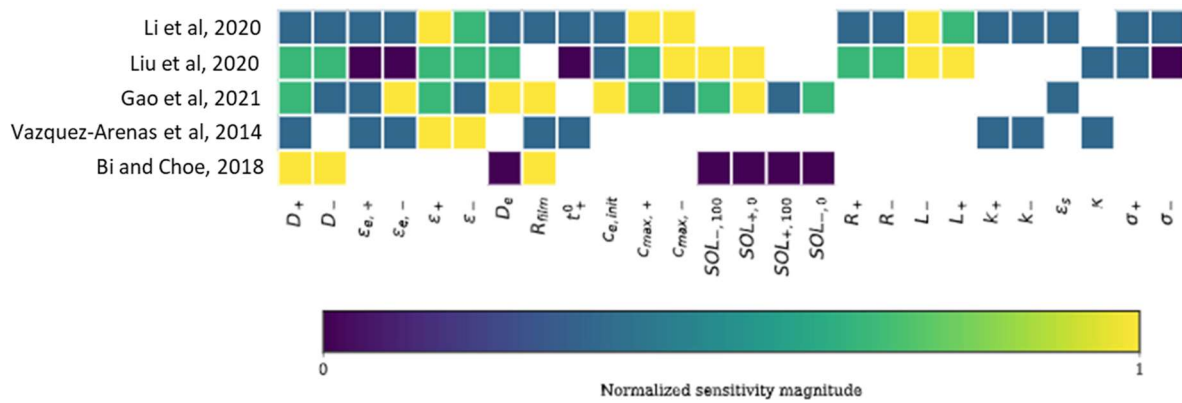


Figure 19: Visual Comparison of different sensitivity analysis weighting magnitude of sensitivity (Andersson et al., 2022)

It is interesting to observe that the different authors weights of most sensitive parameter differ from one another, while performing in a similar PBM environment of the DFN. However, it highlights that different targets of interest and different input drive cycles can influence sensitivity to particular parameters.

While there is no definitive rank that is agreed among these authors, it highlights 6 major parameters that the author can look to perform a separate sensitivity analysis.

- Cathode Thickness (L_p)
- Anode Thickness (L_n)
- Cathode Maximum Ionic Concentration ($C_{p,max}$)
- Cathode Porosity (ϵ_p)
- Anode Porosity (ϵ_n)
- Anode Reaction Rate Coefficient (K_n)

A 2.4 AI methods

Then Andersson et al covers extensively the AI methods that have been deployed to PBM's and summarizes how the methods give the users choice for either fast convergence, high fidelity for global optima or fewer iterations required (Figure 20).

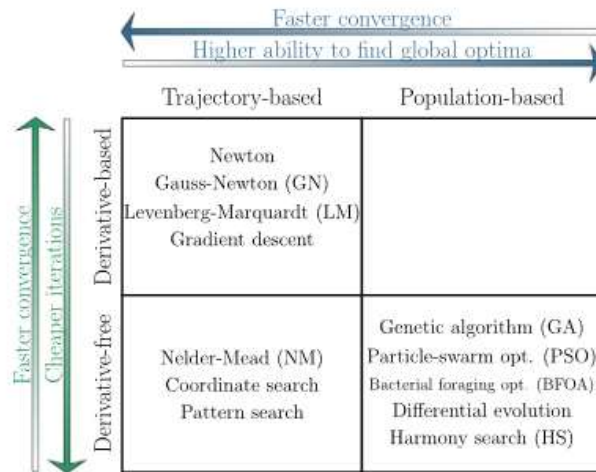


Figure 20: Classification of a subset of optimization methods that has been used for PBM (Andersson et al., 2022)

From the journal, the author identified 5 potential papers that interested the author to explore on how well the models performed and what differentiates them from one another:

- DFN with GA (Li et al., 2022)
- SPM_e with PSO (Fan, 2020)
- DFN with PSO (Rahman, Anwar and Izadian, 2016)
- ECM with PSO-LM (Shen and Li, 2017)
- SPM/DFN with LM (Santhanagopalan, Guo and White, 2007)

Li et al's paper focused on 20 parameters in two steps using a CSA method, optimising the most sensitive 7 parameters first then optimising the remaining in a second set with the first identified parameters (Figure 4). Li et al was able to achieve an RMSE of 10mV-12.7mV which outperformed the experimental dataset of an RMSE between 31.4mV-50.1mV for a 2C discharge case and WLTP, the time taken to achieve these results was 15 hours using 26 cores which is a huge amount of computational resource and time. Li et al's paper reflected that "A major step would be analysing the sensitivity of the thermal and physical parameters to voltage and temperature measurement" (Li et al., 2022).

Fan's paper focused on the 26 parameters in two steps using a PSO method, which targeted 20 parameters in the first step, then 6 parameters focusing on the activation energy. Fan's paper was able to achieve an RMSE of 14.1-33.4mV for the US06, DST and BJDST drive cycle compared to real measured data at 45°C and 0°C. Fan concluded that the RMSE increase is due to extending the study to include more temperature conditions, but was all achieved within 74 mins using a 40 core system (Fan, 2020).

Rahman et al's paper focused on just 4 parameters for both the diffusivity of solid electrodes (D_s) and electrode reaction rates (K), this was achieved by deploying a PSO method. Rahman et al's focused on objectifying the RMSE voltage for both a healthy battery cell and over-discharge battery cell with the AI method, this shows good visual correlation for terminal voltage and shows the powerfulness of using PBM's to target degradation models (Rahman, Anwar and Izadian, 2016).

Shen and Li's paper focused on 7 fitment parameters for an empirical Electrical model, using a PSO-LM method to perform a global and local search pattern to obtain an optimal fitness of terminal voltage. Shen and Li explained the difficulty of building the Jacobian matrix even for 7 parameters so this deterred the author from following this method. Regardless, Shen and Li was able to get good fitment to a 3C charge but did not publish any data regarding RMSE values (Shen and Li, 2017).

Santhanagopalan et al's paper focused on 5 parameters of a hybrid SPM and DFN model, using a LM method to locally search the optimal fitness for terminal voltage performance. Again the paper explains the difficulty of building the Jacobian matrix to drive the optimisation for terminal voltage and only presented the graphical fitment, rather than publishing the RMSE voltage, again this further deterred the author from embarking into the LM method due to the sheer complexity (Santhanagopalan, Guo and White, 2007).

Summarizing the reviewed methods, the PSO method is the fastest method computationally and can provide good fitment when compared to a GA, while a GA can provide a solution which converges faster and to a better resolution. However, the author wishes to utilise the minimized computational time and resource to ensure it is not a hinderance for other users to use the developed toolbox.

A.3 Methodology

The appendix methodology is divided into three sections outlining in greater detail the boundary conditions needed for the OAT analysis (A 3.1), the equations required to drive the PETLION environment for the LGM50 (A 3.2) and the PSO method initialization (A 3.3).

Seen in Figure 21 is the process in how the OAT sensitivity operates within Julia.

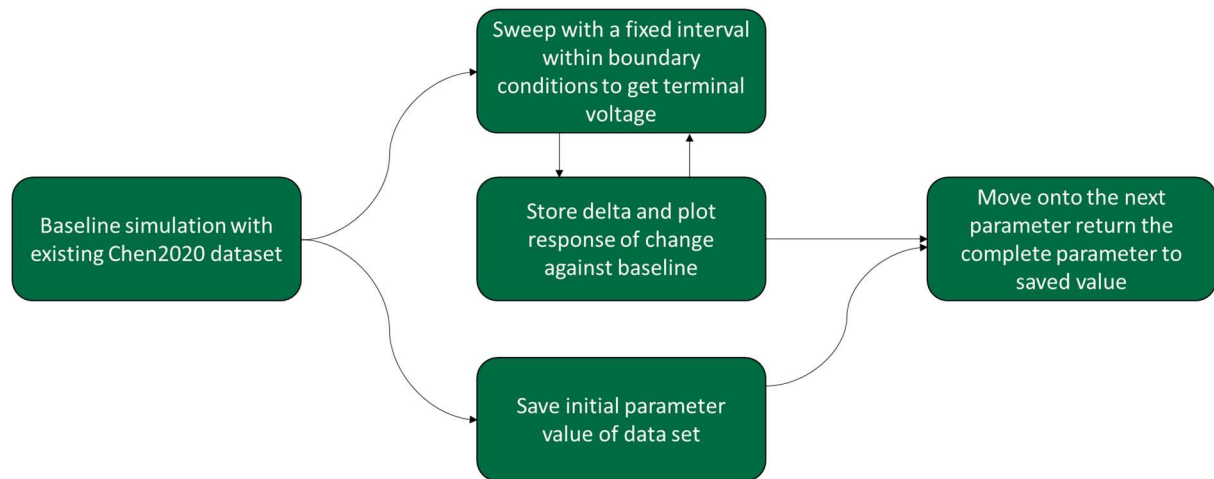


Figure 21: Process for OAT sensitivity analysis

Table 5: Accessed Software tools summary

Package / Database	Code Language	Overall Concept	Positives	Negatives
PETLION (Berliner <i>et al.</i> , 2021)	Julia	<p>High-performance simulations of the pseudo-2D porous electrode theory (PET) model in Julia</p> <ul style="list-style-type: none"> Built for efficient controls, parameter estimation, and other complex battery simulations using the rigorous PET model Runs a full charge or discharge with 301 DAEs in ~3 ms on a laptop with 1 MB total memory usage Includes thermal and aging modes 	<ul style="list-style-type: none"> Fastest solving speed with lowest requirements (22 times faster than PyBaMM, 38 times faster than LIONSIMBA) Thermal analysis model P2D DFN model 	<ul style="list-style-type: none"> Smaller community to PyBaMM so code-based problems are slower to fix. Author has to develop more features for drive cycles, sensitivity and cell parameter sets. Overall, less features to PyBaMM
PyBaMM (Sulzer <i>et al.</i> , 2021)	Python (*Julia via PyCall)	<p>PyBaMM (Python Battery Mathematical Modelling) solves physics-based electrochemical DAE models by using state-of-the-art automatic differentiation and numerical solvers.</p> <ul style="list-style-type: none"> The Doyle-Fuller-Newman model can be solved in under 0.1 seconds, while the reduced-order Single Particle Model and Single Particle Model with electrolyte can be solved in just a few milliseconds. Additional physics can easily be included such as thermal effects, fast particle diffusion, 3D effects, and more. All models are implemented in a flexible manner, and a wide range of models and parameter sets (NCA, NMC, LiCoO₂, ...) are available. There is also functionality to simulate any set of experimental instructions, such as CCCV or GITT, or specify drive cycles. 	<ul style="list-style-type: none"> Fast solving speed for multiple models (~113ms) Wide range of cell datasets to use SPM and SPMe models included with a P2D DFN model Drive cycle analysis methods included Large active coding community and backing for the project, so plenty of help debugging issues. 	<ul style="list-style-type: none"> Slower solving speed to PETLION Julia PyBaMM via PyCall is still in development so bug fixes required and will have a slower computational speed due to pulling request through PyCall

LIONSIMBA (Torchio <i>et al.</i> , 2016)	MATLAB	LIONSIMBA provides a simulation environment for Li-ion cells. The specific modelling approach uses electrochemical pseudo two-dimensional (P2D) model which is represented by means of Partial Differential and Algebraic Equations (PDAEs).	<ul style="list-style-type: none"> • P2D DFN model for PBM • Open-source access to the code itself 	<ul style="list-style-type: none"> • Slowest solving time of ~463ms for a full solution • Using a code base which is not open source, so potentially less adoption in research. • Model cannot be reused for different drive cycle cases • No features for aging • Very small community of users, so debugging potentially was harder.
ARTISTIC (Lombardo <i>et al.</i> , 2022)	Online	The tool links several cell manufacturing parameters and the resulting electrode microstructure. The models used account for three main steps of electrode manufacturing: the slurry phase, drying, and electrode calendaring. All microstructures generated through the platform are shared among all users, making the platform an open and collaborative database linking manufacturing conditions and simulated electrode microstructures.	<ul style="list-style-type: none"> • Highly advanced methods for simulating electrode behaviour in 3D • Plenty of methods accounting for calendar aging to determine electrode behaviour • A platform that does not require any coding experience to obtain high level data. • Large community of high-level industry and universities contributing data openly. 	<ul style="list-style-type: none"> • No real correlation to optimising a P2D DFN or SPM model, solely just electrode level studies • If data was useful an API would have to be built to pull the data across to PBM model.

A 3.1 OAT and Temperature Dependency

The boundary conditions Li et al's identified were then implemented to the authors chosen 6 strong parameters for the OAT (Table 6)

Table 6: Proposed boundary conditions for PETLION OAT for 6 strongest parameters

Parameter	Unit	Boundary Condition	Max Step size
Cathode Thickness (L_p)	m	$[6 \cdot 10^{-5} - 20 \cdot 10^{-5}]$	$1 \cdot 10^{-6}$
Cathode Porosity (ϵ_p)	-	$[0.3 - 0.5]$	0.001
Anode Thickness (L_n)	m	$[6 \cdot 10^{-5} - 20 \cdot 10^{-5}]$	$1 \cdot 10^{-6}$
Anode Reaction Rate Coefficient (K_n)	$m^{2.5}mol^{0.5}s$	$[1 \cdot 10^{-11} - 20 \cdot 10^{-11}]$	$1 \cdot 10^{-12}$
Cathode Maximum Ionic Concentration ($C_{p,max}$)	$mol\ m^{-3}$	$[4.8 \cdot 10^4 - 5.2 \cdot 10^4]$	100
Anode Porosity (ϵ_n)	-	$[0.2 - 0.5]$	0.001

The LCO dataset pre-built into PETLION has $\frac{\partial U}{\partial T}$ which allows the input of temperature to influence the Over Potential curves for both the positive and negative electrodes, these functions are fit using polynomial fitment from measured data. For the LGM50 this has been completed for different temperature conditions, which is what the O'regan2022 dataset accomplishes (O'Regan *et al.*, 2022) (3)(4).

$$\frac{\partial U_p}{\partial T}(x) = a_1 \cdot \exp\left(-\frac{(x - b_1)^2}{c_1}\right) + a_2 \cdot \exp\left(-\frac{(x - b_2)^2}{c_2}\right) \quad (3)$$

$$\frac{\partial U_n}{\partial T}(x) = a_0 \cdot x + b_0 + a_1 \cdot \exp\left(-\frac{(x - b_1)^2}{c_1}\right) \quad (4)$$

This is the prime disadvantage with using the Chen2020 dataset as it does not include temperature dependency to terminal voltage, so this the reason why the author will not complete a temperature dependency study due to wanting to focus solely on parameter identification, which the Chen2020 dataset is excellent benchmark for this. Additionally, Chen et al saw voltage RMSE's between 36-46mV for complete discharge events in their P2D models so this dataset can be considered as a helping benchmark for the PSO to look to optimise further (Chen *et al.*, 2020).

A 3.2 Equations and data for LGM50 into PETLION

The equations required to populate PETLIONS DFN for the Chen2020 dataset are listed below (5)-(7). In order to build an OCV curve it requires to be fitted as a function of the stoichiometry (x) between the lithium concentration of electrode (c_s) against the maximum lithium concentration of electrode (c_s^{max}) which is shown below:

$$x = \frac{c_s}{c_s^{max}} \quad (5)$$

Inputting stoichiometry for the positive electrode into (6) gives the profile of the positive electrode (Chen *et al.*, 2020, p. 202):

$$U_+(x) = -0.8090x + 4.4875 - 0.0428 \cdot \tanh(18.5138(x - 0.5542)) - 17.7326 \cdot \tanh(15.7890(x - 0.3117)) + 17.5842 \cdot \tanh(15.9308(x - 0.3120)) \quad (6)$$

Inputting stoichiometry for the negative electrode into (7) gives the profile of the negative electrode (Chen *et al.*, 2020, p. 202):

$$U_-(x) = 1.9793 \cdot e^{-39.3631x} + 0.2482 - 0.0909 \cdot \tanh(29.8538(x - 0.1234)) - 0.04478 \cdot \tanh(14.9159(x - 0.2769)) - 0.0205 \cdot \tanh(30.444(x - 0.6103)) \quad (7)$$

Secondly the model requires the electrolyte ionic diffusivity (D_e) to be stated with the reference to the electrolyte concentration (c_e) changes:

$$D_e = 8.794 \cdot 10^{-11} c_e^2 - 3.972 \cdot 10^{-11} c_e^2 + 4.862 \cdot 10^{-10} \quad (8)$$

Finally, the electrolyte ionic conductivity (σ_e) is defined like (8) and uses electrolyte concentration:

$$\sigma_e = 8.794 \cdot 10^{-11} c_e^2 - 3.972 \cdot 10^{-11} c_e^2 + 4.862 \cdot 10^{-10} \quad (9)$$

Summarised in Table 7 is the values and equations to drive PETLIONS DFN for the Chen2020 dataset.

Table 7: Chen2020 parameters required for PETLION DFN

Parameter	Unit	Positive Electrode	Separator	Negative Electrode
Current Collector Thickness	m	$16 \cdot 10^{-6}$	-	$12 \cdot 10^{-6}$
Electrode Thickness	m	$75.6 \cdot 10^{-6}$	$12 \cdot 10^{-6}$	$85.2 \cdot 10^{-6}$
Electrode Length	m	1.58		
Electrode Width	m	$6.5 \cdot 10^{-2}$		
Mean Particle Radius	m	$5.22 \cdot 10^{-6}$	-	$5.86 \cdot 10^{-6}$
Electrolyte Volume Fraction	%	33.5	47	25
Active Material Volume Fraction	%	66.5	-	75
Bruggeman exponent	-	2.43	2.57	2.91
Solid Phase Lithium Diffusivity	$\text{m}^2 \text{s}^{-1}$	$1.48 \cdot 10^{-15}$	-	$1.74 \cdot 10^{-15}$
Solid Phase Electronic Conductivity	S m^{-1}	0.18	-	215
Maximum Concentration	mol m^{-3}	51765	-	29583
Stoichiometry at 0% SOC	-	0.9084	-	0.0279
Stoichiometry at 100%	-	0.2661	-	0.9014
Electrolyte Ionic Diffusivity	$\text{m}^2 \text{s}^{-1}$	Using (8)		
Electrolyte Ionic Conductivity	S m^{-1}	Using (9)		
Transference number	-	-	0.2594	-
Initial Electrolyte Concentration	mol m^{-3}	-	1000	-
Open Circuit Voltage	V	Using (6)	-	Using (7)
Activation Energy	J mol^{-1}	$17.8 \cdot 10^3$	-	$35.0 \cdot 10^3$
Reaction Rate	A m^{-2} $(\text{m}^3 \text{mol}^{-1})^{1.5}$	$3.42 \cdot 10^{-6}$	-	$6.48 \cdot 10^{-6}$

A 3.3 Initialization of PSO

The critical equations that are implemented into the different software packages mentioned in Objective 4 are derived from Kennedy and Eberhart's conceptualisation of the PSO method (J. Kennedy and R. Eberhart, 1995).

$$v_i^k = \omega v_i^k + C_1 r_1 (pbest_i^k - x_i^k) + C_2 r_2 (gbest^k - x_i^k) \quad (10)$$

Equation (10) describes the velocity of the particles with respect to the location (x) of the best particle (pbest) and global best particle (gbest). This uses inertia weighting factors (ω) to increase or slow the overall velocity projection of the particle, the learning rates (C) from the pbest and gbest and r is considered to be process noise which follows a uniform gaussian distribution.

$$x_i^{k+1} = x_i^k + v_i^{k+1} \quad (11)$$

Equation (11) is the update of position for the particle with reference to new velocity determined (10). This happens iteratively to create a generational aspect of the algorithm and find the best fitness to the objective function, which for this paper is the Voltage RMSE (1).

The author recognises that these values could potentially be tuned further to have faster convergence, but the author is more concerned on seeing the overall output of the algorithm in the environment of PETLION, then if there is sufficient time can do further tuning.

A.4 Alternative approaches

Table 8: Alternatives approaches for project objectives

Objective	Summary of Objective	Alternative Approaches	Reason to be rejected
1	Literature review of ECM against P2D modelling	Look to focus on an SPM model which has the trade-off having reduced complexity and overall better fitment to terminal voltage compared to an ECM.	A DFN is the superior model when looking to P2D level studies. So, using a SPM may have less parameters required but comes at the penalty of fidelity of terminal voltage responses at high dynamics which is what the author wants to demonstrate against an ECM.
2	Literature review of different sensitivity analysis	Look to use the Monte Carlo method of random sampling to minimise RMSE which potentially could provide a faster method.	There are more papers demonstrating the OAT approach which will make it easier to identify similarities of the authors discoveries compared to the Monte Carlo Approach which only has one paper.
3	Software tool analysis of physical based battery	Look to build a completely independent PBM model.	This is too ambitious for the author to complete alone and would require a team of high-level personnel to achieve this. There are plenty of good tools available (PETLION and PyBaMM) which have communities of users to solve issues that the author encounters.
4	Literature review of AI and statistical modelling approaches	Use a genetic algorithm rather than using a PSO method, as a genetic algorithm can find results which minimised further than a PSO.	The author wants to utilise a more time and resource efficient algorithm such as the PSO at the potential penalty of a result which could be minimised further.
5	Decision of focus of application of model	Using a motorsport approach which looks to find high fitment to high current demand, which is looking at finding what parameters can be pushed to achieve high dynamics.	This is possible when modelling for a PBM and attempting to get fitness to current as OCV is the true output characteristic of the cell that most academic papers are looking for in parametrisation.
6	Development and validation of AI based physical battery model	Using Python packages due to the wider adoption and use in software engineering compared to Julia.	Julia is specifically built to perform as a Data Science and Machine learning tool versus Python which is more of a general-purpose language. Additionally highlighted in Figure 9 is the benefit of using a Julia designed PBM package which is ~20 times faster than a Python Package.

A.5 Project limitations

Table 9: Overall Project Limitations

Area of Project	Limitation	Potential Changes to Project	Overall Outcome
AI Optimisation method (4.3)	At the conceptualisation of the project there was the intent of building a PSO-LM method which combines a global and local approach for optimisation, but this was too ambitious for the author after diving into the literature analysis of building the needed Jacobian Structure to run it (A 2.4)	If the author can use the PSO within PETLION that would be sufficient to be an artificially focused optimisation tool so would still address the main aims of the projects.	Utilised a PSO method which proved to be very effective
Drive cycles for OAT sensitivity (4.1)	The Author could not get the WLTP drive cycle to be run due to the performance limits of the Linux machine used, this means a potential benchmark tool is lost to compare to literature to truly understand how powerful the OAT tool is.	Ensure more literature can look to support the outcomes of the model for the sensitivity of parameters or include a simpler discharge cycle	Found enough literature to confirm the authors observations in parameter sensitivity without the supporting need of simpler test cycles
AI Optimisation tools (3.4)	Was unable to use Optim.jl which is considered to be the standard for Optimisations tools within Julia, due to having PETLION integration issues.	Look for a contingency Julia package to use instead or change to a pure statistical analysis which would not meet the objectives	Used Metaheuristics.jl for the PSO method, which was able to integrate with PETLION so retained the overall objectives
Timeseries Manipulation (A 6.1)	When down sampling the data of HPPC and GITT it incurred a larger than expected RMSE error in voltage, which made it a less viable option to use for the input of an optimisation	Would completely revisit how to condition the input data for the PSO method with alternative methods such as DTW (A 6.1)	Fortunately, was able to use the WLTP drive cycle which was not affected by down sampling and could run the PSO model for a realistic use case

A.6 Results and discussion

The Appendix results and discussion is divided into three sections, which looks to provide more data and detail for how the test and drive cycles performed in the environment of PETLION to real data (A 6.1), further sensitivity analysis performed within PETLION (A 6.2) and the issues encountered with the PSO method for the PBM (A 6.3).

A 6.1 Drive cycles analysis

As seen in Figure 13 for the GITT drive cycle, the HPPC (Figure 22) and WLTP (Figure 23) drive cycles have been emulated and compared to measured LGM50 data below.

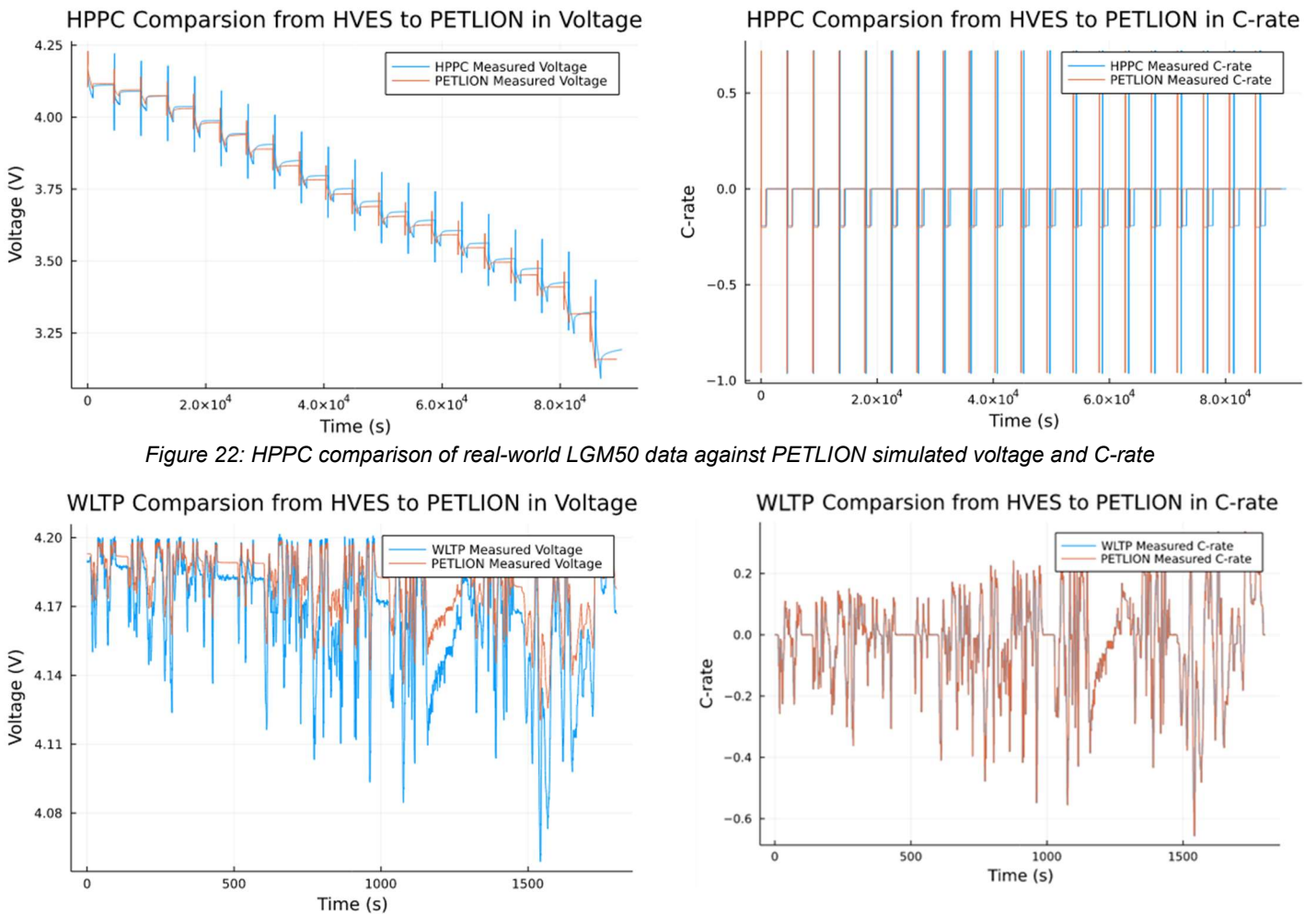


Figure 23: WLTP comparison of real-world LGM50 data against PETLION simulated voltage and C-rate

Figure 22 shows the HPPC test cycle comparison of PETLION's simulated voltage response and the measured LGM50 data, there are some key problems with the voltage profile due to not responding dynamically to the high C pulses and the different timing of pulses seen on the C-rate profile. This is due to the measured HPPC profile being SOC controlled so once the 5% of SOC has been discharged it moves on to the relaxation period irrespective of the time required to remove 5% SOC, whereas PETLION is purely time controlled and used the mean time observed from the measured data for the relaxation period. This explains the large RMSE presented in Table 1 PETLION due to the delay in C-rate deployment. PETLION does have specifiable SOC boundaries within simulate commands, but it is not advanced enough to determine a change in SOC per stage of the HPPC. It is additionally noted that each HPPC simulation takes 4 seconds to complete.

Figure 23 shows the WLTP drive cycle comparison of PETLION's simulated voltage response and the measured LGM50 data, the way this was achieved by using the C-rate profile from the measured LGM50 data for every 500ms, and is input into the simulate function and bounded by the time of drive cycle. This provided an excellent comparison of how the PETLION built DFN responds to measured data as the C-rate profiles are identical. From Table 1 it highlights a good level of RMSE fitment of 16.5mV but there is still some room for improvement at capturing the dynamics in terminal voltage.

The author was surprised with the larger than expected RMSE values for HPPC and GITT, but this is due to the method applied to correlate the datasets as RMSE requires the array lengths to be the same (1) and when plotting the datasets, they have a good level of fit visually. The author used a timeseries focused approach at matching similar events together by timeseries and down sampling the largest array to the smallest array length, this was reasonable for WLTP as that had a continuous time sample.

However, it became problematic for GITT and HPPC as PETLION would only provide data in where significant changes in current or voltage occurred and would stretch the time sample to show the next large event, this is best demonstrated looking at the sampled data of the GITT test cycle for the measured (Down sampled) and PETLION simulated response (Original) (Figure 24).



Figure 24: Time series sampled comparison for GITT, PETLION is original and Measured data is down sampled

As the voltages are miss-matched this greatly effects RMSE, which is the key objective that is being optimised with the PSO. So, using WLTP is preferred as this has a good match to the measured data when sampled for the PSO, but for validation GITT can be used to further demonstrate the ability to minimise a voltage profile.

For the author to improve this aspect of the thesis potentially using Dynamic Time Warping (Müller, 2007) which looks to find the optimal matching of data points from two differently sampled time series. Which could potentially solve this issue and the make input condition more robust and less susceptible to bad fitment.

A 6.2 Sensitivity Analysis

Unfortunately, running the WLTP drive cycle in the OAT condition was not possible, due to exceeding the authors dedicated RAM limits by attempting to store and simulate the true C-rate response of the drive cycle. This was done by allocating the 'simulate!' current control function to be directly fed by the array of the measured data, as per 'simulate!' outputs a minimum of 40 results regardless of time specified, so inputting an array of 4,000 unique C-rate points means in one simulation of a WLTP the data length for a single output variable is ~600,000, then iterating through ~150 OAT points would be ~72MB of memory required for just storing a single variable in a nested loop. This highlighted one key flaw of using a high dynamic drive cycles such as WLTP with the method conceptualised and environment of PETLION, so had to discount the use of WLTP for further OAT analysis due to the values being stored globally via the 'push!' function running out of memory.

Running the GITT and HPPC drive cycles did complete the OAT analysis, however it did present some challenges the author had not foreseen in the initial methodology presented in Figure 21. Within the environment of PETLION allocating a chosen variable to OAT within a function it just physically stored the initial parameter value rather than allowing the model to be influenced by a new value contained within the nested loop, this meant that the item of 'p.θ[:variable]' had to be allocated every time a new variable was simulated rather than caching the initialised 'p.θ'. Which meant the simulations had to have manual changes and reduced the potential to automate the process without the need of an API or Macro.

While in Figure 11b it shows the same behaviours but shows missing datapoints, this is due to the datapoint for temperature producing a terminal voltage response which is not plausible. The check performed for this is ensuring the maximum terminal voltage does not exceed 5V and if a minimum is below 2V. The Author allowed $\pm 0.5V$ on the boundaries for the cells, which gives enough space for high dynamics but can omit 'NaN' for any results which give wildly unrealistic values.

In Figure 25 it shows an example of all the terminal voltage profiles with the influence of L_n being swept from $6 \cdot 10^{-5}$ to $20 \cdot 10^{-5}$.

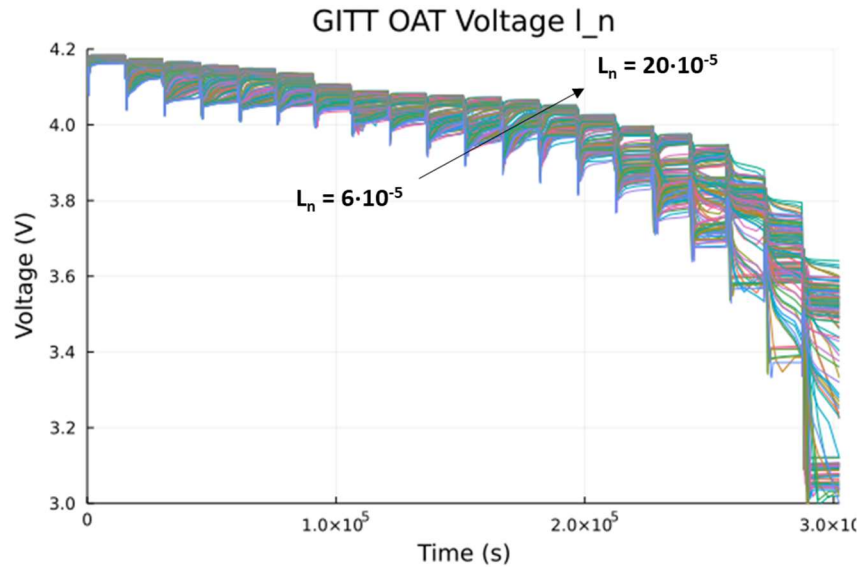


Figure 25: Example of Terminal Voltage changing with OAT L_n

If the author could revisit this aspect of the thesis again, the implementation of attempting to solve more in functions and reducing the need of populating global results, would have improved the ability to allow the WLTP drive cycle to be included in the OAT analysis. Which would have provided an excellent insight into how dynamics can greatly fluctuate RMSE voltage response.

A 6.3 PSO analysis

Continuing from section 4.3 further analysis was conducted on a GITT test cycle. As determined in A 6.1 there is an issue with RMSE being correctly obtained from down sampling data for GITT and HPPC so this primarily is to further prove that the PSO will look to continually reduce RMSE for any voltage profile. This again was run for 3600s with an average function call of 0.2s for a complete GITT cycle with a single core system (Table 10).

Table 10: PETLION PSO results for measure data 'GITT' and WLTP

Parameter	Random Initial guess	RMSE best (mV)	PSO parameter value (GITT)	Percentage difference from Chen2020 (% - GITT)	PSO parameter value (WLTP)	Percentage change GITT to WLTP (%)
Cathode Thickness (L_p)	$9.1 \cdot 10^{-5}$	38.5	$10 \cdot 10^{-5}$	-32.2	$8.05 \cdot 10^{-5}$	19.8
Cathode Porosity (ϵ_p)	0.421		0.5	49.3	0.3	40
Anode Thickness (L_n)	$17 \cdot 10^{-5}$		$10 \cdot 10^{-5}$	3.1	$10 \cdot 10^{-5}$	0
Anode Reaction Rate Coefficient (K_n)	$3.0 \cdot 10^{-11}$		$2.5 \cdot 10^{-11}$	50.3	$2.5 \cdot 10^{-11}$	0
Cathode Maximum Ionic Concentration ($C_{p,max}$)	48741		49754	3.8	52000	-4.5
Anode Porosity (ϵ_n)	0.37		0.2	-1.9	0.2	0

With a 31% improvement on voltage RMSE fitment on the 'Sampled GITT cycle', it is still apparent that regardless of the quality voltage profile the PSO method will find a significantly better fitment for terminal voltage the 6 strongest parameters of a DFN.

A.7 References

- A. M. Bizeray *et al.* (2019) 'Identifiability and Parameter Estimation of the Single Particle Lithium-Ion Battery Model', *IEEE Transactions on Control Systems Technology*, 27(5), pp. 1862–1877. Available at: <https://doi.org/10.1109/TCST.2018.2838097>.
- Andersson, M. *et al.* (2022) 'Parametrization of physics-based battery models from input–output data: A review of methodology and current research', *Journal of Power Sources*, 521, p. 230859. Available at: <https://doi.org/10.1016/j.jpowsour.2021.230859>.
- Berliner, M.D. *et al.* (2021) 'Methods—PETLION: Open-Source Software for Millisecond-Scale Porous Electrode Theory-Based Lithium-Ion Battery Simulations', *Journal of The Electrochemical Society*, 168(9), p. 090504.
- Bezanson, J. *et al.* (2017) 'Julia: A fresh approach to numerical computing', *SIAM Review*, 59(1), pp. 65–98. Available at: <https://doi.org/10.1137/141000671>.
- Chen, C.-H. *et al.* (2020) 'Development of Experimental Techniques for Parameterization of Multi-scale Lithium-ion Battery Models', *Journal of The Electrochemical Society*, 167(8), p. 080534. Available at: <https://doi.org/10.1149/1945-7111/ab9050>.
- Doyle, M., Fuller, T.F. and Newman, J. (1993) 'Modeling of Galvanostatic Charge and Discharge of the Lithium/Polymer/Insertion Cell', *Journal of The Electrochemical Society*, 140(6), pp. 1526–1533. Available at: <https://doi.org/10.1149/1.2221597>.
- Fan, G. (2020) 'Systematic parameter identification of a control-oriented electrochemical battery model and its application for state of charge estimation at various operating conditions', *Journal of Power Sources*, 470, p. 228153. Available at: <https://doi.org/10.1016/j.jpowsour.2020.228153>.
- G. Florentino and M. S. Trimboli (2018) 'Lithium-ion Battery Management Using Physics-based Model Predictive Control and DC-DC Converters', in *2018 IEEE Transportation Electrification Conference and Expo (ITEC). 2018 IEEE Transportation Electrification Conference and Expo (ITEC)*, pp. 916–921. Available at: <https://doi.org/10.1109/ITEC.2018.8450187>.
- Hwang, G. *et al.* (2022) 'Model predictive control of Lithium-ion batteries: Development of optimal charging profile for reduced intracycle capacity fade using an enhanced single particle model (SPM) with first-principled chemical/mechanical degradation mechanisms', *Chemical Engineering Journal*, 435, p. 134768. Available at: <https://doi.org/10.1016/j.cej.2022.134768>.
- J. Kennedy and R. Eberhart (1995) 'Particle swarm optimization', in *Proceedings of ICNN'95 - International Conference on Neural Networks. Proceedings of ICNN'95 - International Conference on Neural Networks*, pp. 1942–1948 vol.4. Available at: <https://doi.org/10.1109/ICNN.1995.488968>.
- Li, W. *et al.* (2020) 'Parameter sensitivity analysis of electrochemical model-based battery management systems for lithium-ion batteries', *Applied Energy*, 269. Available at: <https://doi.org/10.1016/j.apenergy.2020.115104>.
- Li, W. *et al.* (2022) 'Data-driven systematic parameter identification of an electrochemical model for lithium-ion batteries with artificial intelligence', *Energy Storage Materials*, 44, pp. 557–570. Available at: <https://doi.org/10.1016/j.ensm.2021.10.023>.
- Liu, Y. *et al.* (2020) 'Simulation and parameter identification based on electrochemical- thermal coupling model of power lithium ion-battery', *Journal of Alloys and Compounds*, 844, p. 156003. Available at: <https://doi.org/10.1016/j.jallcom.2020.156003>.
- Lombardo, T. *et al.* (2022) 'The ARTISTIC Online Calculator: Exploring the Impact of Lithium-Ion Battery Electrode Manufacturing Parameters Interactively Through Your Browser', *Batteries & Supercaps*, n/a(n/a), p. e202100324. Available at: <https://doi.org/10.1002/batt.202100324>.

Mehta, A. (2022) *Battery boom time*, *Chemistry World*. Available at: <https://www.chemistryworld.com/news/battery-boom-time/4015234.article> (Accessed: 8 November 2022).

Mejía, J. et al. (2022) 'jmejia8/Metaheuristics.jl: v3.2.11'. Zenodo. Available at: <https://doi.org/10.5281/zenodo.7051496>.

Mogensen, P.K. and Riseth, A.N. (2018) 'Optim: A mathematical optimization package for Julia', *Journal of Open Source Software*, 3(24), p. 615. Available at: <https://doi.org/10.21105/joss.00615>.

Müller, M. (ed.) (2007) 'Dynamic Time Warping', in *Information Retrieval for Music and Motion*. Berlin, Heidelberg: Springer Berlin Heidelberg, pp. 69–84. Available at: https://doi.org/10.1007/978-3-540-74048-3_4.

O'Regan, K. et al. (2022) 'Thermal-electrochemical parameters of a high energy lithium-ion cylindrical battery', *Electrochimica Acta*, 425, p. 140700. Available at: <https://doi.org/10.1016/j.electacta.2022.140700>.

Planella, F.B. et al. (2022) 'A continuum of physics-based lithium-ion battery models reviewed', *Progress in Energy*, 4(4), p. 042003. Available at: <https://doi.org/10.1088/2516-1083/ac7d31>.

Plett, G.L., , (2015) *Battery management systems. Volume I, Volume I*. Available at: <https://app.knovel.com/hotlink/toc/id:kpBMSVBM02/battery-management-systems/battery-management-systems>.

Pyswarm, (2022) 'Pyswarm PSO'. Available at: <https://pythonhosted.org/pyswarm/>.

Rahman, M., Anwar, S. and Izadian, A. (2016) 'Electrochemical model parameter identification of a lithium-ion battery using particle swarm optimization method', *Journal of Power Sources*, 307, pp. 86–97. Available at: <https://doi.org/10.1016/j.jpowsour.2015.12.083>.

Santhanagopalan, S., Guo, Q. and White, R.E. (2007) 'Parameter Estimation and Model Discrimination for a Lithium-Ion Cell', *Journal of The Electrochemical Society*, 154(3), p. A198. Available at: <https://doi.org/10.1149/1.2422896>.

Shen, W.-J. and Li, H.-X. (2017) 'Multi-Scale Parameter Identification of Lithium-Ion Battery Electric Models Using a PSO-LM Algorithm', *Energies*, 10(4). Available at: <https://doi.org/10.3390/en10040432>.

Sulzer, V. et al. (2021) 'Python Battery Mathematical Modelling (PyBaMM)', *Journal of Open Research Software*, 9(1), p. 14. Available at: <https://doi.org/10.5334/jors.309>.

Synopsys (2022) 'What is a Battery Management System (BMS)? ♦ How it Works | Synopsys', *Synopsys.com*. Available at: <https://www.synopsys.com/glossary/what-is-a-battery-management-system.html>.

Torchio, M. et al. (2016) 'LIONSIMBA: A Matlab Framework Based on a Finite Volume Model Suitable for Li-Ion Battery Design, Simulation, and Control', *Journal of The Electrochemical Society*, 163(7), pp. A1192–A1205. Available at: <https://doi.org/10.1149/2.0291607jes>.

Vazquez-Arenas, J. et al. (2014) 'A rapid estimation and sensitivity analysis of parameters describing the behavior of commercial Li-ion batteries including thermal analysis', *Energy Conversion and Management*, 87, pp. 472–482. Available at: <https://doi.org/10.1016/j.enconman.2014.06.076>.

Wang, K. (2017) 'Study on Low Temperature Performance of Li Ion Battery', 4, pp. 1–12. Available at: <https://doi.org/10.4236/oalib.1104036>.

X. -S. Yang and Suash Deb (2009) 'Cuckoo Search via Lévy flights', in *2009 World Congress on Nature & Biologically Inspired Computing (NaBIC)*. 2009 World Congress on Nature & Biologically

Inspired Computing (NaBIC), pp. 210–214. Available at: <https://doi.org/10.1109/NABIC.2009.5393690>.

Y. Bi and S. -Y. Choe (2018) 'Automatic Estimation of Parameters of a Reduced Order Electrochemical Model for Lithium-Ion Batteries at the Beginning-of-Life', in *2018 IEEE Vehicle Power and Propulsion Conference (VPPC)*. *2018 IEEE Vehicle Power and Propulsion Conference (VPPC)*, pp. 1–6. Available at: <https://doi.org/10.1109/VPPC.2018.8604954>.

Y. Gao *et al.* (2021) 'Global Parameter Sensitivity Analysis of Electrochemical Model for Lithium-Ion Batteries Considering Aging', *IEEE/ASME Transactions on Mechatronics*, 26(3), pp. 1283–1294. Available at: <https://doi.org/10.1109/TMECH.2021.3067923>.

Zhang, L. *et al.* (2017) 'Comparative Research on RC Equivalent Circuit Models for Lithium-Ion Batteries of Electric Vehicles', *Applied Sciences*, 7, p. 1002. Available at: <https://doi.org/10.3390/app7101002>.

Zhang, R., Xia, B., Li, B., Cao, L., *et al.* (2018) 'State of the Art of Lithium-Ion Battery SOC Estimation for Electrical Vehicles', *Energies*, 11, p. 1820. Available at: <https://doi.org/10.3390/en11071820>.

Zhang, R., Xia, B., Li, B., Lai, Y., *et al.* (2018) 'Study on the Characteristics of a High Capacity Nickel Manganese Cobalt Oxide (NMC) Lithium-Ion Battery—An Experimental Investigation', *Energies*, 11, p. 2275. Available at: <https://doi.org/10.3390/en11092275>.

A.8 Bibliography

Plett, G.L., , (2015) *Battery management systems. Volume I, Volume I.* Available at: <https://app.knovel.com/hotlink/toc/id:kpBMSVBM02/battery-management-systems/battery-management-systems>.